

AD-A251 744



2

OFFICE OF NAVAL RESEARCH

Contract N00014-91-J-1910

R & T Code 4131025

Technical Report #45

DTIC  
ELECTE  
JUN 16 1992  
S A D

The Redox Chemistry of Metallophthalocyanines in Solution

By

E.R. Milaeva, G. Speier and A.B.P. Lever\*

in

The Phthalocyanines, Properties and Applications - Volume 2

York University  
Department of Chemistry, 4700 Keele St., North York  
Ontario, Canada M3J 1P3

Reproduction in whole, or in part, is permitted for any purpose of the United States Government

\*This document has been approved for public release and sale; its distribution is unlimited

\*This statement should also appear in Item 10 of the Document Control Data-DD form 1473. Copies of the form available from cognizant contract administrator

92-15417



92 6 12 021

## REPORT DOCUMENTATION PAGE

1a. REPORT SECURITY CLASSIFICATION			1b. RESTRICTIVE MARKINGS		
2a. SECURITY CLASSIFICATION AUTHORITY Unclassified			3. DISTRIBUTION/AVAILABILITY OF REPORT As it appears on the report		
2b. DECLASSIFICATION/DOWNGRADING SCHEDULE					
4. PERFORMING ORGANIZATION REPORT NUMBER(S) Report # 45			5. MONITORING ORGANIZATION REPORT NUMBER(S)		
6a. NAME OF PERFORMING ORGANIZATION A.B.P. Lever, York University Chemistry Department		6b. OFFICE SYMBOL (if applicable)	7a. NAME OF MONITORING ORGANIZATION Office of Naval Research		
6c. ADDRESS (City, State, and ZIP Code) 4700 Keele St., North York, Ontario M3J 1P3 Canada			7b. ADDRESS (City, State, and ZIP Code) Chemistry Division 800 N. Quincy Street Arlington, VA 22217 U.S.A.		
8a. NAME OF FUNDING/SPONSORING ORGANIZATION		8b. OFFICE SYMBOL (if applicable)	9. PROCUREMENT INSTRUMENT IDENTIFICATION NUMBER N00014-91-J-1910		
8c. ADDRESS (City, State, and ZIP Code)			10. SOURCE OF FUNDING NUMBERS		
			PROGRAM ELEMENT NO.	PROJECT NO.	TASK NO.
			WORK UNIT ACCESSION NO.		
11. TITLE (Include Security Classification) The Redox Chemistry of Metallophthalocyanines in Solution					
12. PERSONAL AUTHOR(S) E.R. Milaeva, G. Speier and A.B.P. Lever*					
13a. TYPE OF REPORT Technical		13b. TIME COVERED FROM June '91 to May '92		14. DATE OF REPORT (Year, Month, Day) May 19, 1992	
				15. PAGE COUNT 67	
16. SUPPLEMENTARY NOTATION					
17. COSATI CODES			18. SUBJECT TERMS (Continue on reverse if necessary and identify by block number)		
FIELD	GROUP	SUB-GROUP			
			Phthalocyanine, Electrochemistry		
19. ABSTRACT (Continue on reverse if necessary and identify by block number)  See attached sheets.					
20. DISTRIBUTION/AVAILABILITY OF ABSTRACT <input checked="" type="checkbox"/> UNCLASSIFIED/UNLIMITED <input type="checkbox"/> SAME AS RPT <input type="checkbox"/> DTIC USERS			21. ABSTRACT SECURITY CLASSIFICATION Unclassified/unlimited		
22a. NAME OF RESPONSIBLE INDIVIDUAL Dr. Ronald A. De Marco			22b. TELEPHONE (Include Area Code)		22c. OFFICE SYMBOL

TECHNICAL REPORT DISTRIBUTION LIST - GENERAL

Office of Naval Research (2)\*  
Chemistry Division, Code 1113  
800 North Quincy Street  
Arlington, Virginia 22217-5000

Dr. Richard W. Drisko (1)  
Naval Civil Engineering  
Laboratory  
Code L52  
Port Hueneme, CA 93043

Dr. James S. Murday (1)  
Chemistry Division, Code 6100  
Naval Research Laboratory  
Washington, D.C. 20375-5000

Dr. Harold H. Singerman (1)  
David Taylor Research Center  
Code 283  
Annapolis, MD 21402-5067

Dr. Robert Green, Director (1)  
Chemistry Division, Code 385  
Naval Weapons Center  
China Lake, CA 93555-6001

Chief of Naval Research (1)  
Special Assistant for Marine  
Corps Matters  
Code 00MC  
800 North Quincy Street  
Arlington, VA 22217-5000

Dr. Eugene C. Fischer (1)  
Code 2840  
David Taylor Research Center  
Annapolis, MD 21402-5067

Defense Technical Information  
Center (2)  
Building 5, Cameron Station  
Alexandria, VA 22314

Dr. Elek Lindner (1)  
Naval Ocean Systems Center  
Code 52  
San Diego, CA 92152-5000

Commanding Officer (1)  
Naval Weapons Support Center  
Dr. Bernard E. Douda  
Crane, Indiana 47522-5050

Accession For	
NTIS CRA&I	<input checked="checked" type="checkbox"/>
DTIC TAB	<input type="checkbox"/>
Unannounced	<input type="checkbox"/>
Justification	
By	
Distribution /	
Availability Codes	
Dist	Avail and/or Special
A-1	



\* Number of copies to forward

1991

## ABSTRACT DISTRIBUTION LIST

Professor Hector Abruña  
Department of Chemistry  
Cornell University  
Ithaca, NY 14853

Professor C. A. Angell  
Arizona State University  
Department of Chemistry  
Tempe, AZ 85287

Professor Allen Bard  
Department of Chemistry  
University of Texas at Austin  
Austin, TX 78712-1167

Professor Douglas Bennion  
Department of Chemical Engineering  
350 CB  
Birgham Young University  
Provo, UT 84602

Professor Lesser Blum  
Department of Physics  
University of Puerto Rico  
Rio Piedras, PUERTO RICO 00931

Professor Daniel Buttry  
Department of Chemistry  
University of Wyoming  
Laramie, WY 82071

Professor Bruce Dunn  
Departement of Materials Science and Engineering  
University of California, Los Angeles  
Los Angeles, CA 90024

Professor Andrew Ewing  
Department of Chemistry  
152 Davey Laboratory  
Pennsylvania State University  
University Park, PA 16802

Professor Gregory Farrington  
University of Pennsylvania  
Department of Materials Science and Engineering  
3231 Walnut Street  
Philadelphia, Pennsylvania 19104

Professor W. R. Fawcett  
Department of Chemistry  
University of California, Davis  
Davis, CA 95616

Professor Harry Gray  
California Institute of Technology  
127-72  
Pasadena, California 91125

Professor Joel Harris  
Department of Chemistry  
University of Utah  
Salt Lake City, UT 84112

Professor Adam Heller  
Department of Chemical Engineering  
University of Texas at Austin  
Austin, TX 78712-1062

Professor Pat Hendra  
The University  
Southampton SO9 5NH  
ENGLAND

Professor Joseph Hupp  
Department of Chemistry  
Northwestern University  
Evanston, IL 60208

Professor Jiri Janata  
Department of Bioengineering  
University of Utah  
Salt Lake City, UT 84102

Professor A. B. P. Lever  
Department of Chemistry  
York University  
4700 Keele Street  
North York, Ontario M3J 1P3

Professor Nathan S. Lewis  
Division of Chemistry and Chemical Engineering  
California Institute of Technology  
Pasadena, CA 91125

Professor Rudolph Marcus  
Division of Chemistry and Chemical Engineering  
California Institute of Technology  
Pasadena, CA 91125

Professor Charles Martin  
Department of Chemistry  
Colorado State University  
Ft. Collins, CO 80523

Professor Royce W. Murray  
Department of Chemistry  
University of North Carolina at Chapel Hill  
Chapel Hill, NC 27514

Dr. Michael R. Philpott  
IBM Research Division  
Almaden Research Center  
650 Harry Road  
San Jose, CA 95120-6099

Professor B. S. Pons  
Department of Chemistry  
University of Utah  
Salt Lake City, UT 84112

Dr. Debra Rolison  
Code 6170  
Naval Research Laboratory  
Washington, DC 20375-5000

Professor Donald Schleich  
Department of Chemistry  
Polytechnic University  
333 Jay Street  
Brooklyn, NY 11201

Professor Jack Simons  
Department of Chemistry  
University of Utah  
Salt Lake City, UT 84112

Dr. H. Gilbert Smith  
TSI Mason Research Institute  
57 Union Street  
Worcester, MA 01608

Professor Eric Stuve  
Department of Chemical Engineering, BF-10  
University of Washington  
Seattle, WA 98195

Dr. Stanislaw Szpak  
Code 634  
Naval Ocean Systems Center  
San Diego, CA 92152-5000

Professor Petr Vanýsek  
Department of Chemistry  
Northern Illinois University  
DeKalb, IL 60115

Professor Michael Weaver  
Department of Chemistry  
Purdue University  
West Lafayette, IN 49707

Professor Henry White  
Department of Chem. Eng. and  
Materials Science  
421 Washington Ave., SE  
University of Minnesota  
Minneapolis, MN 55455

Professor. Mark Wightman  
Department of Chemistry  
University of North Carolina  
Chapel Hill, NC 27599-1350

Professor George Wilson  
Department of Chemistry  
University of Kansas  
Lawrence, KS 66045

Professor Mark S. Wrighton  
Department of Chemistry  
Massachusetts Institute of Technology  
Cambridge, MA 02139

Professor Ernest Yeager  
Case Center for Electrochemical Sciences  
Case Western Reserve University  
Cleveland, OH 44106

# **THE REDOX CHEMISTRY OF METALLOPHTHALOCYANINES IN SOLUTION**

**A. B. P. Lever,<sup>a</sup> Elena R.  
Milaevab, and Gabor Speier<sup>c</sup>**

<sup>a</sup>Department of Chemistry, York University, North York, Ontario, Canada

<sup>b</sup>Department of Organic Chemistry, Moscow State University, Moscow, USSR;

<sup>c</sup>Department of Organic Chemistry, University of Veszprem, 8201 Veszprem,  
Hungary.



- A. Introduction
- B. The Electronic Structure of Metallophthalocyanine Species
- C. Main Group Phthalocyanine Electrochemistry
  - i. Metal Free Phthalocyanines
  - ii. The Alkali Metal Phthalocyanines
  - iii. The Alkaline Earth Metal Phthalocyanines
  - iv. Aluminum, Gallium, Indium, and Thallium Phthalocyanines
  - v. Germanium, Silicon, and Tin Phthalocyanines
  - vi. Phosphorus, Arsenic, Antimony, and Bismuth Phthalocyanines
  - vii. Zinc Phthalocyanines
  - viii. Cadmium, Mercury, and Lead Phthalocyanines
- D. Redox Inactive Transition Metal Phthalocyanines
  - i. Titanium and Vanadium Phthalocyanines
  - ii. Nickel, Palladium, Platinum, and Copper Phthalocyanines
- E. Redox Active Transition Metal Phthalocyanines
  - i. General Introduction
  - ii. Chromium, Molybdenum and Tungsten Phthalocyanines
  - iii. Manganese, Technetium, and Rhenium Phthalocyanines
  - iv. Iron, Ruthenium, and Osmium Phthalocyanines
  - v. Cobalt, Rhodium, and Iridium Phthalocyanines
  - vi. Silver and Gold Phthalocyanines
  - vii. Polynuclear Metal Phthalocyanines
  - viii. Mixed-Valence Behavior
  - ix. Hammett Relationships
- F. Conclusion
- References

---

## A. Introduction

Metallophthalocyanines (MPcs) have a number of characteristic properties that contribute in a major way to their extraordinary versatility. These include their intense color, redox activity, high thermal stability, and non-toxicity. Ultimately, this research will lead to a place in the emerging field of molecular electronics [1]. Actual and potential applications include photoconductive surfaces, optical information storage media, electrochromic devices, analytical (sensor) devices for industrial, environmental and medical applications, molecular metals, batteries, and electrocatalytic and photocatalytic processes including solar energy conversion and production of chemical materials.

Most of the applications rely critically upon the redox properties of MPc species. The Pc unit is an  $18\pi$  electron aromatic system that, in its common oxidation state carries two negative charges. This will be designated Pc(-2) [2]. This unit is capable of oxidation or reduction [3-5]; thus oxidation by one or two-electrons yields Pc(-1) and Pc(0), while reduction by one to four electrons forms Pc(-3), Pc(-4), Pc(-5) and Pc(-6). The central metal ion may be incapable of a redox process in the usual electrochemical regime [most main group species and certain transition metal species such as Ni(II), Cu(II), etc.] or may be a transition element that undergoes oxidation or reduction at potentials comparable to the Pc ring processes.

Many MPc systems bind one or two axial ligands; such coordination can have a major effect upon the observed redox activity [6-12]. Such species are designated here as LMPc or  $L_2$ MPc, where the placing of L ahead of M implies L binding axially to the central metal M.

Most unsubstituted MPc species have only very limited solubility in virtually all solvents, thereby limiting solution phase redox measurements. However, MgPc is rather more soluble as are many transition metal phthalocyanines that dissolve in donor solvents through an axial interaction between the metal center and the donor solvent. This last statement applies especially to those central metal ions that strongly prefer six-coordination rather than four coordination. Thus, for example, iron(II) and cobalt(II) phthalocyanines are soluble in a wide range of donor solvents, while copper(II) phthalocyanine is very much less soluble.

Ring substitution has proved to be a very effective procedure for rendering these substituted MPc species very soluble in a range of solvents, to an extent that, of course, depends upon the substituents used. Even with such species, additional solubility is conferred by axially coordinating central ions. This has led to systems that are extremely soluble in many organic solvents, for example, the tetraneopentoxypthalocyanines [13] or in water, for example, the tetrasulfonated phthalocyanines [14] [see Table 11, above list of references, for the abbreviations used in this chapter].

It is our intent, in this chapter, to organize and systematize the redox properties of a large number of MPc species. To facilitate this organization, data will be reported versus the standard calomel electrode (SCE). However, actual studies have utilized a wide range of reference electrodes, including internal references such as the ferricenium/ferrocene couple. Table 1 lists these various electrodes and indicates the correction made in this chapter to adjust potentials versus SCE. Such adjustments are subject to some error depending upon the quality of the reference electrode, internal resistance problems etc.

Many phthalocyanines aggregate to a greater or lesser extent, both in water and organic phase. Such aggregation is influenced by pH, ionic strength, temperature, the amount of electrolyte in solution, etc. [15-18]. Thus care must be taken in distinguishing redox potentials arising from mononuclear MPc species, and from aggregated species. Aggregation is also influenced by the net charge on the MPc unit, being more important with positively charged species than negatively charged ones. Six coordinate MPc species generally do not aggregate because they are kept apart by the axially bound ligands.

The redox properties may be influenced by different axial ligands attached to the metal center. This can be a very important factor in transition metal MPc chemistry, since many transition metal ions will prefer six-coordination and will bind a donor solvent if no other ligands are competing. Thus the redox chemistry in donor, potentially axially binding solvents, can be very different from that of the same MPc species in a nondonor solvent such as dichlorobenzene.

Even although the metal ion in main group phthalocyanines does not possess partially filled d orbitals, the coordination number for these ions can be more than four; indeed a four coordinate planar environment is very unusual for a main group ion. Thus these main group species may also bind additional ligands or coordinating (donor) solvents, forming five- or six-coordinate species in solution. Such binding can influence the observed redox potentials.

Commonly used nondonor solvents that can dissolve MPc species to a sufficient extent, include o-dichlorobenzene (DCB) and dichloroethane (DCE), and in some early studies, nitrobenzene ( $\text{NO}_2\text{Ph}$ ), chloronaphthalene (ClNap), and 1-methylnaphthalene (MeNp); this last solvent was generally used at  $150^\circ\text{C}$ . Dichloromethane ( $\text{CH}_2\text{Cl}_2$ ) can also be used for the more organic soluble substituted MPc systems such as tetra-t-butylPc (TBuPc) or tetraneopentoxypc (TNPc). More commonly used donor and potentially coordinating solvents include pyridine (Py), dimethylformamide (DMF), dimethylacetamide (DMA), dimethylsulfoxide (DMSO) and benzonitrile (PhCN), all of which tend to be rather good solvents for MPc species even unsubstituted ones, if they, in fact, coordinate to the central ion. Thus, for example, pyridine is a good solvent for  $\text{Co(II)Pc}$ , with which it coordinates, while it is a poor solvent for  $\text{Ni(II)Pc}$  with which it will not coordinate. With any of the solvents listed, extreme care should be taken to ensure that the solvent is dry, if high quality and wide potential range data are sought. In the context of unsubstituted MPc chemistry, the word good

conveys that the species is sufficiently soluble for spectroscopic and electrochemical study, but this may mean a solubility of the order of  $1 \times 10^{-4}$  M !

Supporting electrolyte anions can also play an important role if they have donor characteristics. Thus the perchlorate and hexafluorophosphate ions are usually regarded as nondonor species, although this may not always be absolutely true. Halide ions, on the other hand, especially the commonly employed chloride ion may influence the redox properties dramatically if they axially coordinate.

Although early electrochemical measurements were carried out polarographically using dropping or hanging mercury electrodes, most modern electrochemistry employs solid electrodes, usually platinum or graphite, and cyclic voltammetry (CV) or differential pulse voltammetry (DPV). These last two techniques provide a very rapid assessment of the electrochemical properties of the MPc species. Their analysis can usually rapidly establish whether the electron transfer is electrochemically reversible, or not, and whether there are coupled chemical reactions involved. In general, ring reduction processes are often electrochemically reversible, while ring oxidation processes, especially that associated with  $Pc(0)/Pc(-1)$ , are often irreversible.

It is not the purpose of this chapter to pursue in detail the electrochemical characteristics of the various redox processes except where the Authors concerned have explored such avenues. The reader is referred to an electrochemical text, for example, Bard and Faulkner [19], for the background to such analysis.

Lanthanide diphthalocyanines will not be dealt with in detail in this chapter, since they are considered in Chapter 5 in this volume [20]. Further, the electrocatalytic properties of metallophthalocyanines towards reactive species such as oxygen, hydrazine, sulfides and mercaptans, that involve a significant body of research will be covered in a later volume in this series.

One could pursue the comparative electrochemistry of the phthalocyanines with their cousins the porphyrins. Such a comparison would have greatly increased the length of this contribution. The interested reader is referred to several important reviews of porphyrin electrochemistry [21-23]. Suffice it to say that there are quite close similarities in the gross behavior of both series of complexes. In general, the lower basicity of the phthalocyanines relative to the porphyrins results in the greater stabilization of the lower oxidation states in the former.

In other words, the higher oxidation states of central transition metal ions are more readily accessible in the porphyrin series than in the phthalocyanine series, or, where formed, higher oxidation state metallophthalocyanines are stronger oxidizing agents than their porphyrin analogues.

Table 1 Reference Electrode Corrections to the Standard Calomel Electrode (SCE).

Electrode used	Correction
NHE	-0.24 V
AgCl/Cl	-0.045 V
Fc <sup>+</sup> /Fc	+0.425 V (CH <sub>3</sub> CN) <sup>a</sup>
.	+0.49 V (DCB,DCE) [47]
.	+0.40 V (DMF)
.	+0.50 V (Py, DMSO) [97]
.	+0.45 V (CH <sub>2</sub> Cl <sub>2</sub> ) [75,69]
.	+0.47 V (DMA) [46]
AgClO <sub>4</sub> /Ag (0.01 M HClO <sub>4</sub> )	+0.47 V (CH <sub>2</sub> Cl <sub>2</sub> ) [75]

<sup>a</sup> Our laboratory experience is that the ferrocenium/ferrocene correction is best set at 0.425 V versus SCE in acetonitrile.

## B. The Electronic Structure of Metallo-phthalocyanine Species

The metallophthalocyanines belong to the point group  $D_{4h}$ . The electronic structure of MPc was described by Gouterman and co-workers [24-28] and discussed in depth by Stillman and Nyokong in volume 1 of this series [29]. The HOMO level is  $1a_{1u}(\pi)$ , the next low lying filled orbital is  $1a_{2u}(\pi)$ . The LUMO orbital is  $1e_g(\pi^*)$  and the next is  $1b_{1u}(\pi^*)$  (Figure 1). Transitions from the two upper filled  $\pi$  orbitals to  $1e_g(\pi^*)$  yield the so-called Q (near 600-750 nm) and Soret (or B)  $\pi \rightarrow \pi^*$  (near 300-450 nm) transitions. These both involve an  ${}^1E_u$  excited state, but they are not significantly mixed (unlike the situation in the porphyrin series) because the  $1a_{1u}$  and  $1a_{2u}$  orbitals are fairly well separated in energy. For a complete analysis see the earlier discussion by Stillman and Nyokong [29]. In main group Pcs the redox activity is directly associated, in oxidation, by the successive removal of the electrons from the HOMO,  $1a_{1u}$ , while up to four additional electrons are readily added to  $1e_g$  (LUMO) (reduction), terminating in the Pc(-6) species. The Pc(-3), Pc(-4), Pc(-5) and Pc(-6) ring reduced species have the ground state electron configurations  $(a_{1u})^2 e_g$ ,  $S = 1/2$ ;  $(a_{1u})^2 (e_g)^2$ ,  $S = 0$ ;  $(a_{1u})^2 (e_g)^3$ ,  $S = 1/2$ ; and  $(a_{1u})^2 (e_g)^4$ ,  $S = 0$ , respectively. The Pc(-3) and Pc(-5) ions with an uneven number of electrons show paramagnetism [32] as free radical anions of the phthalocyanine ligand at g factors near that of the free-electron.

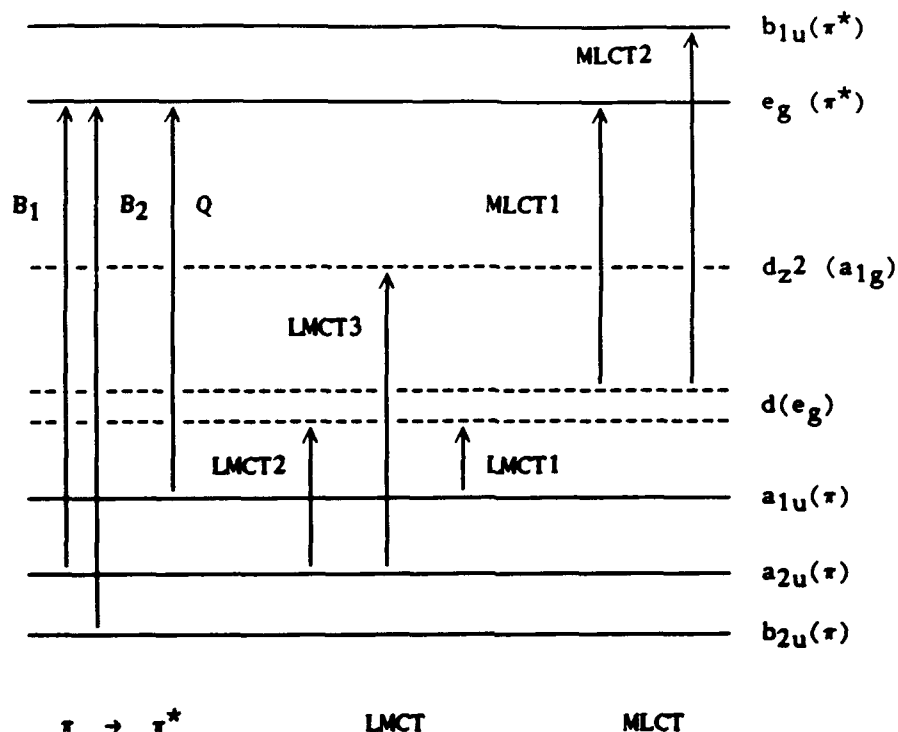


Figure 1 The conventional scheme of the energy levels in MPc and the various transitions (Q, Soret, LMCT, MLCT bands) [7,26-28,30,31].

The ground state for the Pc(-4) species, as an open shell, could be expected to be a triplet, but experimental investigation has shown it to be a singlet [32]. With diamagnetic central ions such as Mg(II), Ni(II), the Pc(-4) species shows no ESR spectrum, but with paramagnetic species such as Co(II) [32] and Cu(II) [32,33] the ESR spectrum characteristic of the central ion itself is observed. If the Pc(-4) species were in fact an  $S = 1$  fragment, then coupling, for example, to the Cu(II) center would yield either a  $S = 3/2$  species (that would not give a typical Cu(II) type spectrum) or, via coupling, an  $S = 1/2$  species, but centered on the Pc ring, giving rise to a free radical spectrum. Thus the Pc(-4) species is likely  $S = 0$ . However, some anomalies in the spacing of the successive reduction processes, for some metal ions, may suggest that the Pc(-4) is not always  $S = 0$ , but can, with some central ions, be  $S = 1$ . The first two reduction processes are generally separated by about 0.4 - 0.5 V (see, for example, Figure 2). With electropositive central ions such as

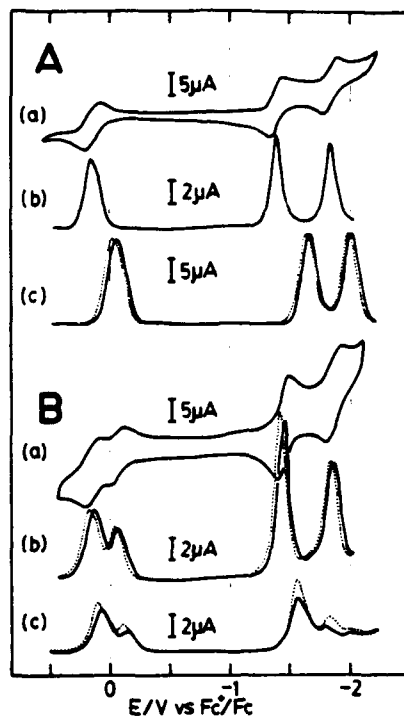


Figure 2 Cyclic and or differential pulse voltammetry of A)  $\text{Zn}[\text{TNPc}(-2)]$  and B)  $\text{Ant}[\text{ZnTrNPc}(-2)]_2$  in DMF (curves a and b) and in DCB (curves c). Scan rates 100 mV/s for cyclic voltammetry, and 5 mV/s for differential pulse voltammetry (DPV). In the DPV curves, the solid and dotted lines indicate cathodic and anodic scans respectively. Reproduced with permission from Ref. [126].

hydrogen or magnesium, the third reduction occurs some 0.8 V more negative than the second. However, with more polarizing central metal ions, the separation is smaller,  $\sim 0.5 - 0.6$  V for  $\text{Zn(II)}$  (but see  $\text{Zn(II)Pc}$  discussion to follow) and as low as 0.4 V for  $\text{Al(III)}$ . It increases to about 0.8 V again for  $\text{Ni(II)}$  and  $\text{Cu(II)}$ . The fourth reduction is usually observed some 0.4 - 0.5 V negative of the third process.

The redox properties of the transition metal phthalocyanines differ from those of main group MPc due to the fact that metal d levels may be positioned between the HOMO ( $\pi$ ) and LUMO ( $\pi^*$ ) orbitals of the phthalocyanine ligand. This has the spectroscopic consequence that one or more metal to ligand (MLCT), or ligand to metal (LMCT) charge-transfer transitions may be

observed in the visible or the near-infrared region [7].

The redox consequence is that oxidation or reduction of the metal may occur at potentials similar to those of ring oxidation or reduction. It is important also to recognize that such internal metal redox processes greatly influence the potentials for ring redox. Thus, for example, the ring oxidation of a species such as  $\text{Co(II)Pc(-2)}$  (to  $[\text{Co(II)Pc(-1)}]^+$ ) will lie at a significantly less positive potential than the oxidation of  $[\text{Co(III)Pc(-2)}]^+$  to  $[\text{Co(III)Pc(-1)}]^{2+}$  (see the following) due to polarization of the phthalocyanine ring by the oxidized metal center.

The oxidized or reduced phthalocyanine species with an uneven number of electrons in the ligand and a diamagnetic metal center exhibit ESR signals due to paramagnetism and therefore can be examined by ESR spectroscopy. Such species generally show a narrow signal at  $g \approx 2.0$  near the free-electron  $g$  value, characteristic of organic free radicals. For example, the  $\text{Pc(-1)}$  species has a configuration  $(1a_{1u})^1$ . Hyperfine structure is not usually observed on these signals because of the extensive delocalization of the spin density in the phthalocyanine ring and relaxation due to aggregation.

In characterizing Pc anion or cation radicals by ESR spectroscopy, care should be taken in evaluating the presence of a free radical ESR signal because many diamagnetic phthalocyanine compounds show a weak ESR signal at  $g = 2.0$  in neutral (not oxidized or reduced) form in the solid state and sometimes in solution. The origin of the ESR signal in these phthalocyanines was discussed by several authors [34-40] in terms of impurities, broken  $\pi$  bonds or defect structures. The dependence of the number of radical species in diamagnetic MPC and the intensity of the ESR signal in the presence of molecular oxygen leads to the belief [41] that the appearance of paramagnetism is a charge-transfer interaction between the phthalocyanine molecule and dioxygen. Thus the ESR signals for MPC and free, unmetallated phthalocyanine are attributed to partial oxidation of the phthalocyanine ring [42].

## C. Main Group Phthalocyanine Electrochemistry

For main group phthalocyanines the first ring oxidation is separated from the first ring reduction by approximately 1.5 V (Table 2) which corresponds approximately to the magnitude of energy difference between the HOMO and LUMO [6,43] (except for metal ions positioned out of the macrocycle plane, for example,  $\text{Pb}^{2+}$ ,  $\text{Hg}^{2+}$ ,  $\text{Cd}^{2+}$ ). However, the individual potentials for the first ring reduction and first ring oxidation do vary remarkably and indeed are functions of the polarizing power of the central metal ion, expressed as charge/radius ( $ze/r$ ). In general the more polarizing the central metal ions, the



Table 2 Main Group and Transition Group Phthalocyanines Exhibiting Redox Processes occurring at the Ring Alone, the Metal Center remaining Invariant. (versus SCE)

Processes	I	II	III	IV	V	VI	Solv.	Ref.
<b>Main Group MPc Species</b>								
$\text{Pc}^{2-}(\text{PrA}^-)_2$			-1.24	-1.55	1.95	-2.19	DMF	4
$\text{H}_2\text{Pc}$		0.64	-0.72				DMF	104
$\text{H}_2\text{Pc}$			-0.66	-1.06	-1.93	-2.23	DMF	4
$\text{H}_2\text{[TNPc]}$			-0.93	-1.31			DCB	47
$\text{H}_2\text{[TNPc]}$	1.38	0.9 <sub>irr</sub>	-0.90	-1.20			DCB	48
$\text{H}_2\text{[TNPc]}$	1.26	0.77	-0.86	-1.21			DCB	49
$\text{H}_2\text{[TBuPc]}$		0.81					PhCN	50
		0.71					$\text{PhNO}_2$	51
			-0.7				DMSO	52, 50
	0.94	0.62	-0.82	-1.19			$\text{CH}_2\text{Cl}_2$	53
			-0.72	-1.13			$\text{CH}_2\text{Cl}_2$	52 <sup>b</sup>
			-0.61	-1.10			MeN/150 <sup>o</sup>	52
$\text{H}_2\text{[TAPc]}$			-0.93	-1.34			DMF	137
$\text{H}_2\text{[TsPc]}$		0.90 <sup>c</sup>	-0.53	-0.97	-1.81		DMSO	5, 54
$\text{H}_2\text{[OCNPc]}$			-0.1	-0.45	-0.88	-1.50	DMF	33, 55
$\text{TDBA[LiPc]}^-$			0.17	-1.37			DMF	56
$\text{Li}_2\text{Pc}$			0.24	0.11 <sup>d</sup>			Acetone	57
$\text{Li}_2\text{Pc}$	1.0	0.17	-1.53				THF/CINap	58
$\text{NaPc}$			-1.06				DMF	104
$\text{Mg(II)Pc}$	1.26	0.65	-0.92	-1.26			DMF	43
			-0.91	-1.39	-2.14	-2.58	DMF	4

Processes	I	II	III	IV	V	VI	Solv.	Ref.
Mg(II)Pc		0.59	-0.99				DMF	56
Mg(II)Pc	1.26	0.61	-0.96				DMF	59
Mg(II)Pc		0.70	-0.95				CINap	60
Mg(II)Pc	1.11	0.65	-0.90	-1.39			DMA	46
Mg(II)Pc			-0.97	-1.44			MeNp/150°	52
TDBA[FMg(II)Pc]⁻		0.50	-1.10				DMF	56
(Im)₂Mg(II)Pc	1.10	0.64	-0.93	-1.47			DMA	46
(MeIm)₂Mg(II)Pc	1.21	0.64	-0.92	-1.39			DMA	46
(Py)₂Mg(II)Pc	1.16	0.67	-0.91	-1.45			DMA	46
		0.70	-0.95				DMF	54
(MePy)₂Mg(II)Pc	1.13	0.67	-0.82	-1.29			DMA	46
Mg(II)[TBuPc]		0.67					PbCN	50
			-0.84				DMSO	50
			-1.15				CH₂Cl₂	52 <sup>b</sup>
			-1.04				MeNp/150°	52
Ba(II)Pc	0.77	0.45	-0.49 <sup>d</sup>				DMF	6
			-1.08				DMF	6
Zn(II)Pc		0.67	-0.86	-1.30	-1.85	-2.25	DMF	55
Zn(II)Pc			-0.89	-1.33	-2.06	-2.68	DMF	4
Zn(II)Pc		0.67	-0.90				DMF	59
Zn(II)Pc		0.64	-0.94				DMF	56
(Py)₂Zn(II)Pc		0.68	-0.89				Py	61
Zn(II)Pc		0.78	-0.80				DMA	60
Zn(II)Pc		0.68					CINap	62

Processes	I	II	III	IV	V	VI	Solv.	Ref.
Zn(II)Pc		0.76	-0.78	-1.14			MeNp/150°	52
Zn(II)[TsPc]			-0.83	-1.30			DMF	63
Zn(II)[TsPc]			-0.85qr	-1.0qr			H <sub>2</sub> O	64
Zn(II)[TNPC]	1.13	0.47	-1.17	-1.55			DCB	65
Zn(II)[TNPC]		0.45	-1.03	-1.45			DMF	65
Zn(II)[TBuPc]			-0.94	-1.29			CH <sub>2</sub> Cl <sub>2</sub>	52 <sup>b</sup>
Zn(II)[TBuPc]		0.66					PhCN	50
Zn(II)[TBuPc]		0.68	-0.92				DMF	tw
Zn(II)[TBuPc]		0.61					DCB 50, 66, 67	54
Zn(II)[TBuPc]	1.33i	0.71	-0.88				DMF	54
Zn(II)[TBuPc]		0.34					PhNO <sub>2</sub>	51
Zn(II)[TBuPc]			-0.96				DMSO	50, 52
Zn(II)[OCNPC]		0.75	-0.83	-1.21			MeNp/150°	52
Zn(II)[OBuxPc]		0.50	-0.15	-0.50	-1.10	-1.35	DMF	33, 55
Zn(II)[Cl <sub>16</sub> Pc]			-1.06	-1.53			DMF(Py)	68
TDBA[FZn(II)Pc] <sup>-</sup>			-0.5	-0.8			DMF	63
Cd(II)Pc	0.88	0.51	-1.06				DMF	56
Hg(II)Pc		0.54	-1.17				DMF	43, 59
Pb(II)Pc		0.25	-1.30				DMF	43
		0.67	-0.82	-1.11			DMSO	104
	0.95	0.65	-0.75	-1.04	-1.92		DMF	9
ClAl(III)Pc			-0.53	-0.98	-1.42	-1.98	DMF	4
ClAl(III)Pc		0.91	-0.66				DMF	104
		0.89	-0.695				DMF	56

Processes	I	II	III	IV	V	VI	Solv.	Ref.
ClAl(III)Pc		0.94	-0.66				DMF	59
ClAl(III)Pc		1.15	-0.50				ClNap	60
(TDBA) <sub>2</sub> [F <sub>2</sub> Al(III)Pc <sub>2</sub> O] <sup>2-</sup>	0.87	0.47	-0.99				DMF	56
TDBA[F <sub>2</sub> Al(III)Pc] <sup>-</sup>		0.69	-0.99				DMF	56
ClGa(III)Pc		0.86	-0.74	-1.14			DMF	6, 43
ClGa(III)[TBuPc]		0.99					PhCN	50
ClIn(III)Pc		0.83	-0.72	-0.95			DMF	43
ClIn(III)[TBuPc]		0.9					PhCN	50
((n-C <sub>6</sub> H <sub>13</sub> ) <sub>3</sub> SiO) <sub>2</sub> Si(IV)Pc <sup>e</sup>		1.00	-0.90	-1.48			CH <sub>2</sub> Cl <sub>2</sub>	69
(O <sup>-t</sup> Amyl) <sub>2</sub> Si(IV)Pc			-0.54	-1.14			DMF	43
<u>Transition metals (non-redox active)</u>								
OTi(IV)[TBuPc]		0.85	-0.515	-1.02			DMF	6
OV(IV)[TBuPc]		0.94	-0.58	-1.08			DMF	6
Ni(II)Pc		1.05					ClNap	62
Ni(II)Pc			-0.85	-1.23	-2.01	-2.35	DMF <sup>a</sup>	4
Ni(II)Pc			-0.72	-1.20			MeNp/150°	52
Ni(II)[TsPc]		0.95	-0.71	-1.14			DMF	6
Ni(II)[TsPc]			-0.67	-1.13			DMSO	64
Ni(II)[TsPc]				-1.34 <sup>c</sup> irr			H <sub>2</sub> O	64
Ni(II)[TBuPc]		0.67					PhNO <sub>2</sub>	51
		1.06	-0.89				DMF	54
			-0.85				DMSO	52
			-0.89	-1.31			CH <sub>2</sub> Cl <sub>2</sub>	52 <sup>b</sup>

Processes	I	II	III	IV	V	VI	Solv.	Ref.
Ni(II)[TBPc]			-0.76	-1.24			MeNp/150°	52
Ni(II)[TAPc]		0.23 <sup>8</sup>	-1.00	-1.45			DMSO	70
Cu(II)Pc		0.98					ClNap	62
Cu(II)Pc			-0.84	-1.18	-2.01	-2.28	DMF <sup>1</sup>	4
Cu(II)Pc			-0.70	-1.14			MeNp/150°	52
Cu(II)[DsPc]			-0.79	-1.18			DMSO	64
Cu(II)[DsPc]				-1.10 <sup>c</sup>	-1.25ads		H <sub>2</sub> O	64
Cu(II)[TsPc]		0.87 <sup>c</sup>	-0.745	-1.14			DMF	6
Cu(II)[TsPc]		0.84	-0.84				DMF	56
Cu(II)[TNPc]			-0.88	-1.26			DCE	47
Cu(II)[TBPc]		0.64	-0.91	-1.34			PhNO <sub>2</sub>	51
							DMF	tw
		0.87					DCB	66
			-0.86	-1.26			CH <sub>2</sub> Cl <sub>2</sub>	52 <sup>b</sup>
			-0.81				DMSO	52
			-0.74	-1.18			MeNp/150°	52
			-0.89				DMF	6
			-0.2	-0.63	-1.08	-1.25	DMF	33, 55
Cu(II)[OCNPc]							ACN	71
Cu(II)[TcPc]		1.26					DCB	47
Me <sub>2</sub> O(5)[Cu(II)TrNPc] <sub>2</sub>		0.82		-1.04	-1.31		PhNO <sub>2</sub>	51
Pd(II)[TBPc]		0.72					MeNp/150°	52
Pt(II)Pc			-0.67	-1.05			PhNO <sub>2</sub>	51
Pt(II)[TBPc]		0.73					PhNO <sub>2</sub>	51
Py(CO)Ru(II)Pc		0.87					CH <sub>2</sub> Cl <sub>2</sub>	12

Processes	I	II	III	IV	V	VI	Solv.	Ref.
$\text{Py}_2\text{Ru(II)Pc}$	1.36	0.73					$\text{CH}_2\text{Cl}_2$	12
$(4\text{-MePy})_2\text{Ru(II)Pc}$	1.36	0.71					$\text{CH}_2\text{Cl}_2$	12
$(4\text{-MePy})(\text{CO})\text{Ru(II)Pc}$		0.84					$\text{CH}_2\text{Cl}_2$	12
$(4\text{-BuPy})_2\text{Ru(II)Pc}$	1.28	0.66					$\text{CH}_2\text{Cl}_2$	12
$(\text{CH}_3\text{CN})_2\text{Ru(II)Pc}$		0.68					$\text{CH}_2\text{Cl}_2$	12
$(\text{DMF})_2\text{Ru(II)Pc}$		0.76					$\text{CH}_2\text{Cl}_2$	12
$(\text{DMF})(\text{CO})\text{Ru(II)Pc}$		0.86					$\text{CH}_2\text{Cl}_2$	12
$(\text{DMSO})_2\text{Ru(II)Pc}$		0.85					$\text{CH}_2\text{Cl}_2$	12

<sup>a</sup> Where data have been reported by two laboratories using the same solvent and report numbers agreeing within 20 mV, only the average is cited in the table. The processes are: I  $\text{MPc}(0)/\text{MPc}(-1)$ ; II  $\text{MPc}(-1)/\text{MPc}(-2)$ ; III  $\text{MPc}(-2)/\text{MPc}(-3)$ ; IV  $\text{MPc}(-3)/\text{MPc}(-4)$ ; V  $\text{MPc}(-4)/\text{MPc}(-5)$ ; VI  $\text{MPc}(-5)/\text{MPc}(-6)$ . Charge excluded for clarity. <sup>b</sup> Data reported against  $\text{Fc}^+/\text{Fc}$  internal reference. We have corrected using +0.45 V versus SCE; the authors report 0.55 V but this seems to provide, for the most part, poorer agreement with related data. <sup>c</sup> 2-electron process. <sup>d</sup> Assignment very uncertain since the potential is too close to the next more positive wave. <sup>e</sup> see data for oligomeric silicon Pcs in Table 3. <sup>f</sup>  $\text{Pr}_4\text{NOH}$  supporting electrolyte. <sup>g</sup> authors suggest  $\text{Ni(III)/Ni(II)}$ . See Tables 4 and 5 for further data for zinc phthalocyanines. Axial ligand abbreviations are those commonly used and are not listed. All phthalocyanine, and solvent, abbreviations can be found in Table 11.

easier it is to reduce the ring, and the more difficult to oxidize the ring. A linear plot of these quantities, the first reduction and oxidation potentials versus  $ze/r$ , has been obtained for many MPc species ( $M = Zn^{2+}, Mg^{2+}, In^{3+}, Ga^{3+}, Al^{3+}, Si^{4+}$ ) in DMF [43]

The linear relationships are:

$$E^0_{ox} = 1170 - 11.7 (r/ze)$$

$$E^0_{red} = -385 - 12 (r/ze) \quad (1)$$

for the first oxidation and reduction potentials versus SCE ( $E^0$  in mV,  $r$  in pm using ionic radii from the listing of Shannon and Prewitt [44]).  $Cd(II)$ ,  $Hg(II)$ , and  $Pb(II)Pc$  lie well off these lines as a consequence of being too large to fit well inside the Pc ring. It is certainly true that there will be a similar relationship for transition metal central ions, with the higher oxidation state ions causing more ready ring reduction provided that central metal ion reduction does not occur first (at less negative potentials); however, no explicit linear correlations concerning this prediction have been reported.

Axial ligation has been studied for some main group MPcs, especially magnesium, [8, 45, 46] (Table 2) however, the effects are rather small for the main groups (in contrast to the transition groups where axial ligation can effect large redox potential changes.) Although the axial ligation can be monitored spectroscopically [8, 45], the electrochemical response in the main groups is small.

The low solubility of most main group Pcs has limited the availability of acceptable quality electrochemical data. A few more soluble ring substituted species are available and are cited in Table 2. In general, however, aside from  $Mg$  and  $ZnPc$ , main group MPc solution electrochemistry has been rather neglected.

### i. Metal-Free Phthalocyanines

A range of metal-free Pcs has been explored and all oxidation states between  $[H_2Pc(0)]^{2+}$  and  $[H_2Pc(-5)]^{3-}$  have been reported. The first oxidation and reduction potentials for the variously substituted species fall within fairly narrow ranges (Table 2) with separation of about 1.4 V. However,  $H_2[TNPc]$  in the aromatic solvent DCB, curiously, is a little more difficult to reduce and a little more difficult to oxidize than average, with separation of some 1.6 V. The irreversibility of the first oxidation noted in [48] arises from aggregation effects. The  $Pc(-2)$  anion is present in the propylammonium salt (Table 2) (and also in the lithium salt, see the following) and is more difficult to reduce because of the net negative charge [4].

On the other hand, the octacyano substituted  $H_2[OCNPc]$  is much easier to reduce. Its electrochemistry, however, is somewhat anomalous. The first three reduction potentials are separated by about 0.3 V, a rather small potential gap, especially between the second and third steps; however, the fourth reduction step is displaced some 0.62 V more negative than the third rather than the more usual 0.3 - 0.4 V.

## ii. The Alkali Metal Phthalocyanines

The low solubility and sensitivity to water has precluded many studies of the electrochemistry of these species. It would be advantageous to synthesize organic soluble ring substituted Pc derivatives of these metals; except for  $Li_2[TBuPc]$  [72], such are currently unknown.

The alkali metal complexes provide the interesting example of the dilithium salt [56-58, 73],  $Li_2Pc(-2)$  which would be expected to contain the highly oxidizable  $[Pc(-2)]^{2-}$  anion with electrostatic forces binding the  $Li^+$  ions. Indeed oxidation occurs at only  $\sim 0.15$  V versus SCE, giving the free radical one-electron oxidation product  $LiPc(-1)$ , which is quite a stable species and whose crystal structure has been recorded [73]. A poorly defined wave corresponding to the second oxidation process to  $[LiPc(0)]^+$  has also been reported [58], as has reduction to the first anion radical,  $[Pc(-3)]^{3-}$ , occurring at a significantly more negative potential, as a consequence of excess negative charge [58].

## iii. The Alkaline Earth Metal Phthalocyanines

The heavier metals, Ca, Ba, Sr have hardly been explored and again would bear study as organic soluble species. Magnesium Pc however, has been studied extensively.

$MgPc$  is a nice example of a well-behaved metallophthalocyanine in that the central metal is not redox active and all redox processes therefore occur on the phthalocyanine ring. In all, six redox processes have been observed, spanning  $[MgPc(0)]^{2+}$  to  $[MgPc(-6)]^{4-}$ .

The effect of imidazoles, pyridines, and cyanide as ligands in the six-coordinate  $L_2Mg(II)Pc(-2)$  species ( $L = Py, 4MePy, Im, MeIm, CN^-$ ) on the spectroscopic and redox properties has been studied [46] using electronic absorption, MCD spectroscopy, and electrochemistry in solutions. The axial ligands cause a shift in all absorption bands compared with that of the position of the parent  $Mg(II)Pc$ . The band center energies are red-shifted in a sequence that follows a decrease in the  $\sigma$ -donor and  $\pi$ -acceptor strengths of the ligand:  $H_2O > CN^- > Me-py > py > Me-im > im$ ; however, the overall shifts are very small, of the order of a few hundred wavenumbers. The unligated species will be



axially solvated by solvent donor molecules, and may be coordinated by trace water in nondonor solvents.

However, axial ligands actually have no significant effect upon the ring redox processes exhibited by  $L_2Mg(II)Pc$  (Table 2). This is not peculiar to the hard acid magnesium since, as will be discussed, axial ligation has very little effect upon ring localized redox processes even with transition metal MPc species.

The  $[FMg(II)Pc(-2)]^-$  anion has also been studied [56] and has been shown to be rather more easily oxidized, and somewhat more difficult to reduce than other  $L_2Mg(II)Pc$  systems (Table 2). This suggests significant reduction of the net electropositive nature of the hard  $Mg(II)$  ion by strong binding to fluoride.

Data for  $Ba(II)Pc$  are reported in Table 2. On the basis of the polarizing power of the central ion [43], this species should be easier to oxidize than  $Mg(II)Pc$ , and it is, but it is more difficult to reduce than  $Mg(II)Pc$ . The oxidation potential at 0.45 V is approximately correct as predicted by Eq.(1). Two reduction potentials are reported at -0.49 and -1.08 V [6]. The first is far too positive to be associated with formation of  $[Ba(II)Pc(-3)]^-$  but the second is consistent therewith. The process at -0.49 V must arise from an impurity.

#### iv. Aluminum, Gallium, Indium, and Thallium Phthalocyanines

In line with their greater polarizing power,  $XAl(III)Pc(-2)$  species [4, 56, 59, 60] are easier to reduce than  $Mg(II)Pc(-2)$  but more difficult to oxidize (Table 2). In parallel with the  $[FMg(II)Pc(-2)]^-$  analogue, the  $[F_2Al(III)Pc(-2)]^-$  [56] is relatively easier to oxidize and more difficult to reduce. A binuclear complex,  $[FAl(III)Pc(-2)]_2O$  shows two oxidation processes consistent with formation of a mixed-valence binuclear species (see the following) [56].

$XGa(III)Pc(-2)$  and  $XIn(III)Pc(-2)$  [6, 43, 50] behave analogously to  $XAl(III)Pc(-2)$ . There is no evidence for reduction of the metal to  $Ga(I)$  or  $In(I)Pc(-2)$  species, although canonical contributions of  $XIn(I)Pc(-2)$  to  $XIn(III)Pc(-4)$  could possibly be relevant. Contributions from  $Tl(I)$  could be more important in  $XTl(III)Pc(-2)$  reduction processes, but data are unavailable.

#### v. Germanium, Silicon and Tin Phthalocyanines

No solution data appear available for  $L_2Ge(IV)Pc(-2)$  species.

There have been many papers describing the electrochemistry and electronic structure of monomeric and oligomeric silicon phthalocyanines [43, 69, 74-79]. Data are reported in Table 3 (and shown in Figure 3) appertaining to  $(nC_6H_{13})_3SiO$  derivatives [69], while data for  $t-BuMe_2SiO$  systems [75] are very closely similar and are not reported here. Data for the same  $(nC_6H_{13})_3SiO$

derivatives are also included in [77] reported versus a  $\text{ClO}_4^-$  anodized silver reference electrode. If these are corrected to SCE by normalizing to the data for the monomeric species in [69], then the results for the dimer, trimer and tetramer differ substantially and by a non constant error from those in [69]. However, the individual potential energy differences between successive redox processes agree in both reports, for all species. This lack of agreement can only be explained by assuming that one of the reference systems was drifting from one experiment to the next. Since SCE electrodes are usually drift free, while silver wire electrodes are known to have drift problems, we suppose that the data in [69] are correct, especially as they agree with data for the closely related species in [75].

Although an early report suggested that the first oxidation and reduction waves of the dimer corresponded each with two-electron processes [76], it is now generally agreed that all these processes (Figure 3) are one-electron in nature and therefore that mixed-valence species are generated (see Section E, viii.).

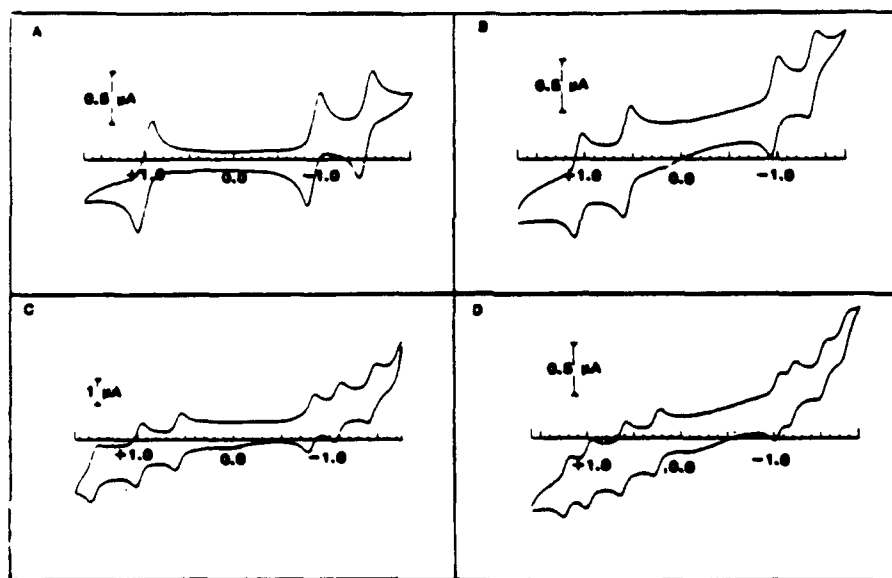


Figure 3 Cyclic voltammetry of oligomeric silicon phthalocyanines,  $(n\text{-C}_6\text{H}_{13})_3\text{SiO}(\text{SiPcO})_n\text{Si}(n\text{-C}_6\text{H}_{13})_3$  ( $n=1\text{-}4$ ) in 0.1 M TBA ( $\text{BF}_4$ ) in dichloromethane. All potentials versus Ag reference electrode. Scan rate 100 mV/s. A) Monomer, B) Dimer, C) Trimer and D) Tetramer. Reproduced with permission from Ref. [69].

It becomes progressively easier both to reduce and to oxidize these species as one proceeds from monomer to dimer to trimer to tetramer (possibly not true for the first reduction of the tetramer), although this effect is more marked for oxidation than reduction. The separation between the first oxidation and reduction waves necessarily decreases in this sequence.

This separation is a measure of the LUMO-HOMO gap, that is evidently decreasing. This is to be expected if both the  $\pi$  and  $\pi^*$  levels of adjacent SiPc rings overlap.

The phthalocyanine rings interact through spatial overlap of the  $\pi$ -orbitals [75, 78, 80], rather than through bonds, as for example in a homologous series of conjugated aromatics. The steady decrease in the first oxidation potential from monomer to tetramer shows a progressive stabilization of the (mono)cation whose charge is probably delocalized to some extent over the oligomeric system. The much smaller effect for the first reduction potential shows that, in contrast, the (mono)anion is not significantly stabilized [75].

Table 3 Silicon Phthalocyanine Oligomers Showing Mixed-Valence Behavior (In Dichloromethane). Species  $(nC_6H_{13})_3SiO(SiPcO)_nSi(n-C_6H_{13})_3$ <sup>a</sup> [69]

	n = 1	n = 2	n = 3	n = 4
4th Oxidation				1.38
3rd Oxidation			1.47	1.15
2nd Oxidation		1.20	1.00	0.79
1st Oxidation	1.00	0.71	0.59	0.43
1st Reduction	-0.90	-0.81	-0.78	-0.84
2nd Reduction	-1.48	-1.21	-1.06	-0.98
3rd Reduction			-1.41	-1.30
4th Reduction				-1.54

<sup>a</sup> Diffusion coefficient values are also included in this report [69].

However, the mean oxidation potential (midway between the 2, 3 and 4 oxidation waves of the dimer, trimer and tetramer, respectively) does not differ significantly from that of the monomer oxidation. This mean potential refers to the free energy for forming the dication of the dimer, the trication of the trimer, and the tetra-cation of the tetramer. Its invariance and similarity to the oxidation potential of the monomer shows that once all the rings have been oxidized by one-electron, there is no net stabilization of the oligomer.

The mean of the first reduction, however, defined in a similar fashion, becomes progressively more negative as oligomerization proceeds (see Figure 3

and also Figure 3 in [75]). Thus the change in free energy for placing a negative charge on each ring of the monomer, dimer etc. is consistent with increasing interelectronic repulsion destabilizing the anion radicals so formed.

Data for t-amylxy silicon phthalocyanine, dissolved in DMF, are also reported in [43] (Table 3). This species appears to be about 300 mV easier to reduce than the  $(n\text{-C}_6\text{H}_{13})_3\text{SiO}$  species as a consequence of the change in axial ligand and/or solvent. This datum fits the polarization plot [43], while a value of about -0.9 V for the first reduction process would be a poor fit to the regression analysis.

#### vi. Phosphorus, Arsenic, Antimony, and Bismuth Phthalocyanines

While species with these central ions are known, little is known about them. Electrochemical studies could prove very interesting.

#### vii. Zinc Phthalocyanines

$\text{Zn(II)Pc}$  species have been the object of intense electrochemical study [33, 48-52, 54-56, 59-68, 81] (Figures 2, 4). As with magnesium, the central ion is well behaved and redox inactive so that all oxidation states from  $[\text{Zn(II)Pc(0)}]^{2+}$  to  $[\text{Zn(II)Pc(-6)}]^{4-}$  are fairly readily observable. Indeed the actual redox potentials are very closely similar to those of  $\text{Mg(II)Pc}$ .

The question of the separation of the second and third reduction process was raised previously. Two data sets [4, 55] for  $\text{Zn(II)Pc}$  in DMF cover the entire reduction region to  $[\text{Zn(II)Pc(-6)}]^{4-}$  but unfortunately the numbers for the third and fourth reduction processes differ quite dramatically in the two reports (Table 2). In terms of the relative separations between successive reduction processes, the data in [55] seem more reliable.

$\text{Zn(II)[TBuPc]}$  has been studied by many workers (see Table 2). Data are fairly consistent, although the datum for oxidation in  $\text{PhNO}_2$  seems too low [51].

Similar to the fluoroaluminum system,  $[\text{FZn(II)Pc(-2)}]^-$  is easier to oxidize and more difficult to reduce than most other  $\text{Zn(II)Pc}$  species. Two other species bear special comment. Data for a series of tetrasubstituted zinc phthalocyanines are shown in Table 4, while similar data for octasubstituted Zinc species are shown in Table 5.

The octacyano species,  $\text{Zn(II)[OCNPc]}$  [33, 55] is very much easier to reduce due to the electron attracting cyano substituents, with reduction processes shifted some 0.8 V more positive than most other  $\text{Zn(II)Pc}$  species. This octacyano species is strongly aggregated in DMF solution, and the aggregation-disaggregation equilibrium is slow relative to the electrochemical

time scale. Thus redox processes due to both aggregated and unaggregated  $Zn(II)[OCNPc]$  can simultaneously be observed [55] (Figure 4, processes 1a,1b), with the aggregated species being reduced first (process 1a). Two different anion species,  $[Zn(II)[OCNPc(-3)]]^-$  can be observed by reduction at -0.1 and -0.3 V showing that the monoanion species also exists as a mixture of aggregated and unaggregated species. The  $Pc(-3)$  and more reduced species are however, disaggregated, probably because of their larger negative charges.

The perchloro species,  $Zn(II)[Cl_{16}Pc(-2)]$  [63] also has its reduction processes shifted dramatically positive, by the electron-withdrawing effect of the chloro substituents, but only by about 0.5 V, rather less than for the octacyano derivative. The low solubility of the perchloro species precludes a very detailed study.

Table 4 Oxidation Potentials of some Ring Tetra-Substituted MPc Species in Dichlorobenzene, except where indicated.

R	$R_4Pc(-1)/R_4Pc(-2)$ Zn(II)	$R_4Pc(-1)/R_4Pc(-2)$ Ref.	Co(II)	Ref.
H			0.86(ACN)	71
			0.845	83
MeO	0.625	82	0.725	83
			0.69(ACN)	71
t-Bu	0.685	82	0.745	83
PhO	0.755	82	0.805	83
Ph	0.755	82	0.835	83
PhS	0.785	82	0.865	83
NH <sub>2</sub>			0.68(ACN)	71
CO <sub>2</sub> H			1.20(ACN)	71
NO <sub>2</sub>			1.26(ACN)	71
Neopentoxy	0.47	65		

#### viii. Cadmium, Mercury, and Lead Phthalocyanines

Another situation arises with phthalocyanines containing cadmium, mercury and lead as the central ion. These compounds show anomalous redox behavior [6, 9, 43]. The ionic radii of these elements are too large to lie within the plane of the phthalocyanine core, and as indicated above, their redox potentials do not adhere to the predictions in Eqs.(1). Since the metal sits outside of the phthalocyanine ring, the complex shows a tendency to demetallation in redox

reactions. This was observed by Kadish and co-workers [9] during the electrochemical reduction of Pb(II)Pc in DMF. There are three successive reversible one-electron reduction steps observable on the cyclic voltammetric time scale. However, if the potential is held just negative of the first reduction (to [Pb(II)Pc(-3)]<sup>-</sup>) then demetallation occurs over a period of minutes, lead metal is deposited onto the electrode and metal-free phthalocyanine (or its anion radical) is generated in solution.

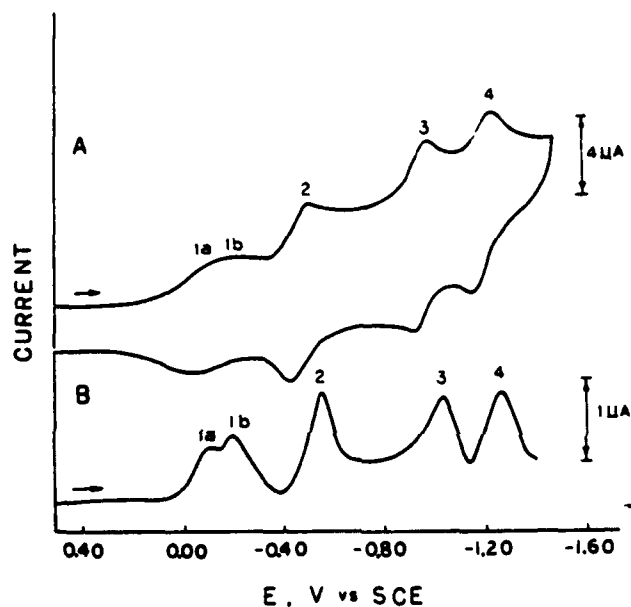


Figure 4 Voltammetry of Zinc Octacyanophthalocyanine ( $5 \times 10^{-4}$  M) [33, 55], at a Hg electrode in DMF/(0.1 M TBAP). A) Cyclic voltammetry, 0.2 V/s; and B) Differential pulse voltammetry at 10 mV/s. Reproduced with permission from Ref. [55].

This behavior is reminiscent of that of Ag(II)TNPc (see the following) that is also demetallated when reduced to Ag(I)[TNPc(-2)], for the same reason. Pb(II)Pc shows two reversible oxidations to the mono- and dication radical species [9].

Table 5 Oxidation Potentials of some Ring Octa-Substituted MPc Species in Acetonitrile.

R	Zn(II)[R <sub>8</sub> Pc(-1)] <sup>+</sup> /Zn(II)[R <sub>8</sub> Pc(-2)]	Ref.	Co(II)[R <sub>8</sub> Pc(-1)] <sup>+</sup> /Co(II)[R <sub>8</sub> Pc(-2)]	Ref.
MeO			0.73	71
Me			0.79	71
CO <sub>2</sub> H			1.61	71
CN			1.76	71
BuO	0.50(DMF)	68		
H	0.67(DMF)	33	0.86	71

## D. Redox Inactive Transition Metal Phthalocyanines

### i) Titanium and Vanadium Phthalocyanines

OTi(IV)Pc [86] is very insoluble in most solvents. Its solution electrochemistry is unknown, but its surface electrochemistry, while not discussed here, has been explored in some detail [87]. It is, however, possible to form organic solvent soluble OM(IV)[TBuPc] species [6]. The central ion is fairly strongly polarizing and somewhat easier to reduce than, say, Ni(II) or Cu(II)Pc (Table 2). However, they are not especially difficult to oxidize. The separation between first oxidation and first reduction, and the separation between the two reduction processes are typical for ring redox processes. Had metal reduction occurred, then successive reduction processes are expected to be separated further (for example, see Co(II), Fe(II) to follow). Moreover, reduction would likely have generated species such as [Ti(III)Pc(-2)]<sup>+</sup> in which the oxide ligand had been reduced off. The electrochemistry would then most probably have been irreversible. Thus, although spectroelectrochemical data were not obtained it would appear that there is no evidence for reduction of the central titanium or vanadium ions, even although these metal ions are normally readily reducible.

No solution data exist for Zr, Nb, Hf, or Ta phthalocyanine species. There is a clear need for further development of organic soluble MPc species of the left-hand period transition elements and elucidation of their electrochemical and photophysical properties. The extensive patent literature for OV(IV)Pc as a potential optical recording agent suggests that such further study would be profitable.

## ii. Nickel, Palladium, Platinum and Copper Phthalocyanines

Ni(II)Pc(-2) behaves rather like Zn(II)Pc(-2); it is slightly more difficult to oxidize, while reduction to the monoanion radical, Pc(-3), occurs at about the same potential [4-6, 51, 52, 54, 62, 70]. No reduction at the central nickel ion is expected although it is theoretically possible.

The aqueous solution chemistry has been explored with Ni(II)[TsPc] which shows, in water, a two-electron first reduction process [64]. The species is strongly aggregated in water.

Ni(II)[TAPc] [70] is more difficult to reduce than most other Ni(II)Pc species, showing a rather more electron-rich tetraamino-phthalocyanine ligand. An oxidation wave is observed only some 1.2 V positive of the first reduction, rather than the more usual  $\approx 1.6$  V. The authors had proposed that this was a Ni(III)/Ni(II) couple; however, ring oxidation is more probable [135]. Oxidation of the corresponding Co(II)[TAPc] occurs at only some 0.69 V positive of the first reduction process and the assignment of oxidation to  $[(\text{DMSO})_2\text{Co(III)TAPc(-2)}]^+$  is almost certainly valid.

Brief details of the reduction of Pd(II)Pc and Pt(II)Pc dissolved in methylnaphthalene at 150°C are reported in Table 2. Little is known of these systems in solution, although surface state electrochemical data for Pt(II)Pc are available [84].

Copper phthalocyanines show well behaved redox processes [4,6, 47, 51, 52, 56, 62, 64, 66] centered on the ligand, from  $[\text{Cu(II)Pc(-1)}]^+$  to  $[\text{Cu(II)Pc(-5)}]^{3-}$  at potentials very similar to those of NiPc. The octacyano species, Cu(II)[OCNPc], as with other such species, shows couples shifted some 0.6 - 0.8 V positive of those of other CuPc species [33, 55].

---

## E. Redox Active Transition Metal Phthalocyanines

### i. General Introduction

If the transition metal ion concerned has no accessible d orbital levels lying within the  $1a_{1u}$  (HOMO) -  $1e_g$  (LUMO) gap of a phthalocyanine species, then its redox chemistry will appear very much like that of a main group species. The nickel, palladium, platinum group behave in this fashion, with the M(II) central ion being unchanged as the MPc unit is either oxidized or reduced. Copper(II) also appears invariant in the MPc framework, with reduction occurring at the ring rather than at the copper ion. Silver however, behaves differently, as will be discussed. However, some species vary their electrochemistry according to their



environment. For example, the oxidation of  $\text{Co(II)Pc(-2)}$  can lead to  $[\text{Co(II)Pc(-1)}]^+$  or  $[\text{Co(III)Pc(-2)}]^+$  depending upon whether there are any available suitable coordinating species that would stabilize the  $\text{Co(II)}$  center; these variations are explored in the following.

When a cyclic voltammogram, such as that shown in Figure 2, for  $\text{Zn(II)[TNPc]}$  is obtained, then, assuming the rest potential [85] is known, the couples are easily assigned to successive ring reductions and ring oxidations of the bulk species. With the corresponding voltammograms for  $\text{Co(II)[TNPc]}$  (Figure 5) containing a metal center that itself may undergo a redox process, the assignment of the couples is no longer straightforward. From knowledge of the rest potential, it is certainly easy to distinguish net reductions of the bulk, from net oxidations, but the voltammogram does not readily convey information about the site of the redox process, metal center, or ring. To solve this dilemma, the usual procedure is to carry out controlled potential reductions some 200 mV negative of each reduction couple, and some 200 mV positive of each oxidation couple, in order to generate solutions containing bulk quantities of the various reduced and oxidized species.

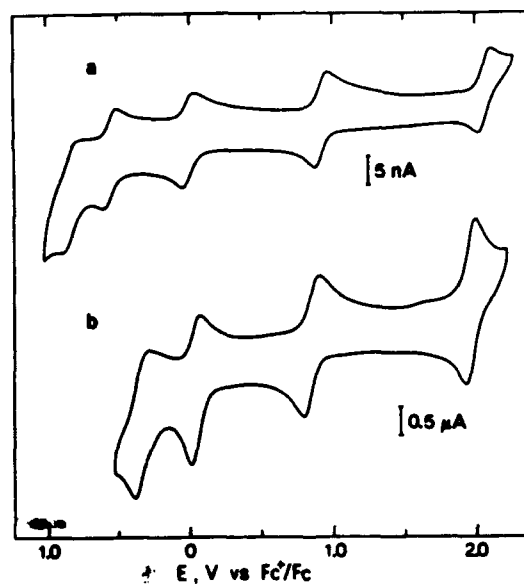


Figure 5 Cyclic voltammetry for  $\text{Co(II)[TNPc(-2)]}$  ( $1 \times 10^{-4}$  M), a) in DCB solution, and b) in DMF solution. Scan rate 50 mV/s,  $[\text{TBAP}] = 0.3$  M. Reproduced with permission from ref. [49].

Table 6 Transition Metal Electrochemistry - Systems Displaying M(III), M(II) and M(I) (versus SCE)<sup>a</sup>

Species	Ring Oxidn Process	Metal centered Process M(III)/M(II)	M(II)/M(I)	Ring Reduction. Processes	Condn.	Ref.
Cr(III)[TsPc]	0.51	-0.40		-1.00	DMF	5,6,54
(Py) <sub>2</sub> Cr(II)Pc	0.95	0.52			Py	61,92a
(Py) <sub>2</sub> Cr(II)Pc		0.63		-0.90	Py/Cl	92a
Na[(CN) <sub>2</sub> Cr(III)Pc]	0.90	-0.56		-1.23	Acetone	88
(HO)Cr(III)[TBuPc]	0.70	-0.87		-1.36	DMF	92a
(HO)OMo(V)[TsPc]		0.51(VI/V)	-0.28(V/IV)		DMF	92b
Mn(II)Pc		-0.08	-0.755		DMSO	93,95
Mn(II)Pc		-0.085	-0.70		DMSO/Br	93
Mn(II)Pc		-0.125	-0.765		DMSO/Cl	93
Mn(II)Pc		0.005	-0.785		Py	93,95
Mn(II)Pc		-0.035	-0.71		Py/Br	93
Mn(II)Pc		-0.105	-0.80		Py/Cl	93
Mn(II)Pc		-0.23			1M Py/CH <sub>2</sub> Cl <sub>2</sub>	
Mn(II)Pc		-0.14	-0.69		DMF	6,60,93
Mn(II)Pc	0.87	-0.14	-0.69	-1.46	DMF	93,95
Mn(II)Pc				-1.50	DMF	4
Mn(II)Pc		-0.115	-0.78	-2.20	DMF/Br	93
Mn(II)Pc		-0.155	-0.80	-2.75	DMF/Cl	93
Mn(II)Pc		-0.13	-0.80		DMA/Br	93
Mn(II)Pc		-0.14	-0.80		DMA/Cl	93
Mn(II)Pc			-0.71	-1.16	MeNp/150°	52

Species	Ring Oxidn Process <sup>a</sup>	Metal centered Process M(III)/M(II)	M(II)/M(I)	Ring Reduction Processes	Condn.	Ref.
Mn(II)[TsPc]			-0.72	-1.36	DMF	5,6,54
Mn(II)[tBuPc]	0.89	-0.13	-0.69		DMF	54
Mn(II)[tBuPc]		-0.115	-0.89		DMF	6
Na[(CN) <sub>2</sub> Mn(III)Pc]	0.89	-0.14	-0.91		Acetone	88
Fe(II)Pc		0.37	-0.55	-1.17	DMA	6,60,93
Fe(II)Pc		0.38	-0.55	-1.17	DMA	95
Fe(II)Pc				-2.05	DMF	4
Fe(II)Pc			-0.70	-1.56	MeNp/150°	52
Fe(II)Pc		0.17	-0.86	-1.13	DMA/Br	97
Fe(II)Pc		-0.15	-0.64	-1.19	DMA/Cl	97
Fe(II)Pc		-0.21		-1.13	Py/OH	106
Fe(II)Pc		0.46	-0.71		DMSO	95,97
Fe(II)Pc		0.39	-0.77		DMSO/Br	97
Fe(II)Pc		0.35	-0.69		DMSO/Cl	97
Fe(II)Pc			-0.74	-1.15	DMSO/ClO <sub>4</sub>	98
Fe(II)Pc			-0.74	-1.14	DMSO/246Coll	98
Fe(II)Pc			-0.80	-1.16	DMSO/24Lut	98
Fe(II)Pc			-0.82	-1.15	DMSO/26Lut	98
Fe(II)Pc			-0.87	-1.20	DMSO/Me <sub>2</sub> Im	98
Fe(II)Pc			-0.93	-1.21	DMSO/3Pic	98
Fe(II)Pc			-0.94	-1.20	DMSO/Melm	98
Fe(II)Pc			-0.95	-1.22	DMSO/Py	98

Fe(II)Pc		-0.99	-1.23	DMSO/4Pic 98
Fe(II)Pc		-1.17	-1.17 <sup>b</sup>	DMSO/NMeIm 98
Fe(II)Pc		-1.21	-1.21 <sup>b</sup>	DMSO/Im 98
Fe(II)Pc	0.66	-1.07		Py 97
Fe(II)Pc	1.10	-1.085	-1.93	Py 107
Fe(II)Pc				CINap 62
Fe(II)Pc				ACN 71
Fe(II)Pc				Acetone 88
[(CN) <sub>2</sub> Fe(III)Pc] <sup>-</sup>	0.93	-0.99	-1.52	CH <sub>2</sub> Cl <sub>2</sub> 100
[(CN) <sub>2</sub> Fe(III)Pc] <sup>-</sup>	0.74			ACN 105
[(CN) <sub>2</sub> Fe(III)Pc] <sup>-</sup>	1.16	-0.247?		Py 137
Fe(II)[OMePc]	0.56	-0.92	-1.45qr	MeNp/150° 52
Fe(II)[TBuPc]		-0.85	-1.16	CH <sub>2</sub> Cl <sub>2</sub> 52
Fe(II)[TBuPc]		-0.95	-1.30	DMSO 52
Fe(II)[TBuPc]		-1.12		ACN 71
Fe(II)[TePc]	1.22			DMF 63
Fe(II)[Cl <sub>16</sub> Pc]			-1.11	DMF 5,6,54
Fe(II)[TsPc]	0.89	-0.74	-1.08	DCB 48
Ag(II)[TNPC]	1.72, 1.19	-0.79i	-1.47	Acetone 88
K <sub>2</sub> [(CN) <sub>2</sub> Ru(II)Pc]	0.93		-0.97	Acetone 88
K[(CN) <sub>2</sub> Rh(III)Pc]	0.90		-0.90	ACN 108
(MeOH)ClRh(III)Pc	0.87			DCB 109
ClRh(III)Pc	0.97	-1.47		

Solvent conditions include "non-coordinating" supporting electrolyte anion, anion except where another anion is specifically cited. ? signifies experimental data are likely correct but their interpretation is doubtful. ?? signifies the data themselves are doubtful. <sup>a</sup> Assignments made by this author do not always agree with those made by the original authors. <sup>b</sup> Two-electron combined couple.

Electronic spectroscopy (including magnetic circular dichroism, MCD) and electron spin resonance (ESR) spectroscopy of these solutions can then usually determine the site of redox. If reduced or oxidized species can be isolated, then other characterization procedures such as FTIR, magnetic susceptibility measurements, and x-ray photoelectron spectroscopy might be employed. Quite frequently the combination of electronic spectra and ESR is sufficient to determine the site of redox especially when studying a metal ion for which there already exists an extensive database.

It is not the purpose of this chapter to delineate in any detail how the distinction between metal centered or ring redox processes can be made. The reader is referred to relevant chapters in these volumes where such information is available.

## ii. Chromium, Molybdenum, and Tungsten Phthalocyanines

Although the chemistry of chromium phthalocyanines has been fairly extensively studied [6, 54, 61, 88-90], their electrochemistry is, as yet, poorly characterized (Table 6). Both  $\text{Cr(II)Pc}$  and  $\text{XCr(III)Pc}$  species are known, with the former being air sensitive. Thus the first reduction process, for  $\text{XCr(III)Pc}$ , is almost certainly  $\text{XCr(III)Pc/Cr(II)Pc}$ . The potential of this first reduction process varies over quite a considerable range  $(-0.87 - (+0.52) \text{ V})$  (Table 6). The most positive potential appears in pyridine wherein  $(\text{Py})_2\text{Cr(II)Pc}$  is known to be formed as a stable, air-insensitive species [90]. The most negative III/II potential refers to the reduction of  $\text{HOCr(III)[TBuPc(-2)]}$  [6, 91] in DMF wherein the species  $(\text{DMF})_2\text{Cr(II)[TBuPc(-2)]}$  is likely formed. The DMF group is likely to stabilize  $\text{Cr(III)}$  to a much greater degree than pyridine consistent with the electrochemical observation. We had previously assigned [6] the potential at  $-0.87 \text{ V}$  to  $\text{Cr(II)Pc(-2)/Cr(II)Pc(-3)}$  but this is unlikely to be correct since one would then have to assign the oxidation at  $+0.7$  to the  $\text{Cr(III)/Cr(II)}$  couple, an unreasonably high value. There is no systematic study of the effect of axial ligation on the potential of the  $\text{Cr(III)/Cr(II)}$  couple, but the potentials for  $(\text{Py})_2\text{Cr(II)Pc}$  and  $(\text{DMF})_2\text{Cr(II)[TBuPc(-2)]}$  (from the hydroxychromium(III) species in DMF) being so disparate  $(+0.52 \text{ and } -0.87 \text{ V})$  would make such a study worthwhile.

Some previously unpublished data [92a] for  $(\text{Py})_2\text{Cr(II)Pc}$  dissolved in pyridine in the presence of chloride ion are reported in Table 6. Unfortunately spectroelectrochemical data were not collected at the time. The presence of chloride ion is expected to favor  $\text{Cr(III)}$ . A couple appears at  $-0.9 \text{ V}$  in the  $(\text{Py})_2\text{Cr(II)Pc/Py/Cl}^-$  system and may involve the  $\text{Cr(III)/Cr(II)}$  couple for a chloride bound species.

Thus the  $\text{Cr(III)/Cr(II)}$  couple appears to vary over an exceptionally wide

range as a function of axial ligand: (Py)<sub>2</sub> 0.52; (CN)<sub>2</sub> -0.56; (DMF)<sub>2</sub> -0.87; Py, Cl<sup>-</sup> -0.90 V. Clearly, further work coupled to spectroelectrochemical data is required.

Further reduction (of Cr(II)Pc(-2)) probably yields a [Cr(II)Pc(-3)]<sup>-</sup> species, while oxidation (of XCr(III)Pc(-2)) almost certainly yields [XCr(III)Pc(-1)]<sup>+</sup> radical cation species, but confirmatory evidence is lacking (Table 6).

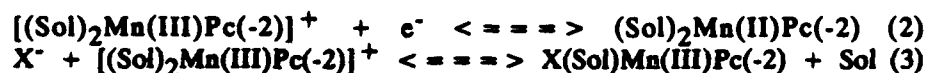
Ferraudi has recently published some solution data for O(HO)Mo(V)[TsPc] in DMF [92b], with the apparent identification of the Mo(VI)/Mo(V) and Mo(V)/Mo(IV) redox couples (Table 6). No solution electrochemical data appear to exist for any tungsten phthalocyanines.

### iii. Manganese, Technetium, and Rhenium Phthalocyanines

Extensive solution data exist for manganese phthalocyanines, but no data for either technetium or rhenium.

The electrochemistry of Mn(II)Pc has been studied in some depth [6, 52, 60, 93-95]. It shows very little variation with coordinating axial ligand (donor solvent or supporting electrolyte anion). The Mn(III)/Mn(II) oxidation couple lies in the narrow range -0.23 - (+0.005) V for all systems studied. There is a slight stabilization of Mn(II) in the sequence Py > DMSO > DMA = DMF [93]. Coordination by strongly coordinating anions favors Mn(III), in the sequence Cl<sup>-</sup> > Br<sup>-</sup> > ClO<sub>4</sub><sup>-</sup> but the variation is much smaller than for iron phthalocyanine (see the following). There is a rather flat, but linear, correlation with the donor number (Gutmann) of the solvent, with a slope the same as that to be discussed below for Fe(III)Pc/Fe(II)Pc [95].

Two equilibria should be considered:



Where Sol is solvent and X<sup>-</sup> is a counteranion, and where six-coordinate Mn(III) is inferred from a solution magnetic susceptibility study [93]. Equilibrium (3) shifts the potential to more negative values with increasing stabilization of the X(Sol)Mn(III)Pc(-2) species. Since [(\text{Sol})<sub>2</sub>Mn(III)Pc(-2)]<sup>+</sup> is easier to reduce than X(Sol)Mn(III)Pc(-2), the equilibrium will shift so as to produce this latter species on the electrode at the reduction couple potential. With high-speed voltammetry one may expect that it should be possible also to see the reduction couple for X(Sol)Mn(III)Pc(-2) if scanning is faster than the rate for re-equilibration to [(\text{Sol})<sub>2</sub>Mn(III)Pc(-2)]<sup>+</sup>. Such an additional couple is seen with X<sup>-</sup> = OH<sup>-</sup> [94], where couples corresponding to the reduction of both Mn(III) species can be observed. Their total reduction current is constant with

respect to scan rate, but the relative ratio of the two currents depends upon scan rate, favoring the  $X(\text{Sol})\text{Mn(III)Pc}(-2)$  species at higher scan rates. The reduction product,  $[\text{HOMn(II)Pc}(-2)]^-$  loses  $\text{OH}^-$ , very rapidly such that its reoxidation is not observed at the highest scan rates studied [94].

A further oxidation couple was only seen in DMF (at +0.87 V) but the product was not stable on spectroelectrochemical oxidation. The couple likely corresponds to  $[\text{XMn(III)Pc}(-1)]^+ / \text{XMn(III)Pc}(-2)$  rather than oxidation to Mn(IV), but spectroelectrochemical evidence is desirable.

The first reduction potential also occurs within a very narrow range (-0.69 - (-0.80) V) being essentially independent of solvent or counteranion. This argues for reduction to the anion radical, viz  $\text{Mn(II)Pc}(-2)/[\text{Mn(II)Pc}(-3)]^-$  rather than to the  $d^6$   $[\text{Mn(I)Pc}(-2)]^-$ , which, by analogy with  $d^6$   $\text{Fe(III)Pc}$ , is expected to show marked solvent and anion dependence. The electronic spectrum of this reduced species is consistent with formation of the anion radical [93].

Smith, Pilbrow and co-workers [96] have studied the chemical reduction products of  $\text{Mn(II)[TsPc}(-2)]$ , and on the basis of ESR spectroscopy, assign the two successive reduction processes to formation of  $\text{Mn(I)[TsPc}(-2)]^-$  and  $\text{Mn(0)[TsPc}(-2)]^{2-}$  (where any charges on the sulfonyl groups are ignored).

While the solvent independence of the first reduction process argues for anion radical formation, the separation between the first and second reduction processes ( $\approx 0.6$  V) is rather large to be ascribed to successive phthalocyanine ring reduction processes that are normally separated by about 0.4 V (see preceding discussion) [4]. The observed separation of 0.77 V (in DMF) is more consistent with the separation of the second and third ring reduced species, but that assumption fails to provide a logical assignment for the -0.7 V couple. If this latter couple is assigned to  $\text{Mn(II)Pc}(-2)/[\text{Mn(I)Pc}(-2)]^-$ , then the separation of 0.77 V to the next reduction process, to form  $[\text{Mn(I)Pc}(-3)]^{2-}$  or  $[\text{Mn(0)Pc}(-2)]^{2-}$ , is not unreasonable, although it is substantially less than the corresponding separation in CoPc chemistry (about 1.1 V, see the following). Note that Clack, Hush and Woolsey [4] quote two further reduction processes, in DMF, whose potentials and separations are consistent with the sequential reduction of the phthalocyanine ring.

In methylnaphthalene at 150°C,  $\text{Mn(II)Pc}$  shows a normal pair of reduction processes [52] separated by 0.45 V. Possibly in noncoordinating solvents, reduction to  $[\text{Mn(II)Pc}(-3)]^-$  takes place, while in coordinating solvents,  $[\text{S}_2\text{Mn(I)Pc}(-2)]^-$  is formed, even although little solvent dependence is observed. A complete understanding of this system remains elusive (data are so-assigned in Table 6).

Manganese phthalocyanine can be oxidized to form a bridging oxo species,  $\text{PcMn(III)-O-Mn(III)Pc}$  whose electrochemistry has been explored in depth [94]. Figure 6 illustrates its intriguing electrochemistry. Detailed analysis of the current of the several couples, as a function of scan rate, reveals that  $\text{PcMn(III)-O-Mn(III)Pc}$  undergoes a two-electron reduction, at -0.85 V, to yield

$[\text{PcMn(II)-O-Mn(II)Pc}]^{2-}$ , which is unstable with respect to bridge cleavage generating two mononuclear  $\text{Mn(II)Pc(-2)}$  fragments. These, however, exist on an electrode polarized (at  $-0.85 \text{ V}$ ) at a potential negative of the reduction process to form  $[\text{Mn(II)Pc(-3)}]^-$ ; thus two further electrons are taken up to form two molecules of this anion radical species. Thus  $\text{PcMn(III)-O-Mn(III)Pc}$  undergoes a four-electron irreversible reduction at this potential. A careful analysis of the high-and low-scan rate data provided evidence for this 2+2 reduction mechanism in distinction to possible alternatives such as a concerted four electron reduction step, or 1+3 combinations [94].

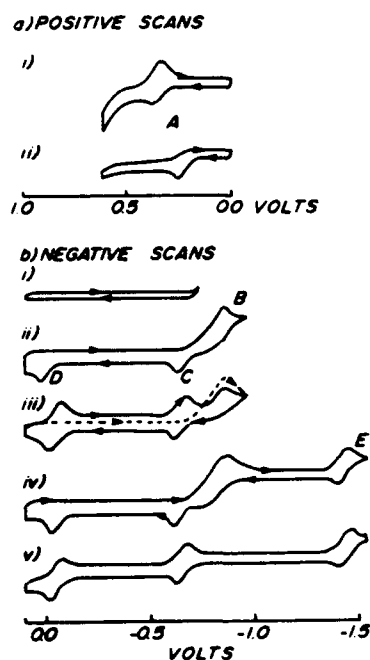


Figure 6 Cyclic Voltammetry of  $\mu$ -oxobis(phthalocyaninemanganese(III)) [94]. a) oxidation in i) pyridine, and ii) DMF. b) Reduction voltammograms in pyridine/TEAP, i) initial scan  $+0.1$  to  $-0.8 \text{ V}$ ; ii) initial scan  $+0.1$  to  $-1.1 \text{ V}$ ; iii) initial (dotted) and second (solid) scans  $+0.1$  to  $-1.1 \text{ V}$ ; iv) initial scan  $+0.1$  to  $-1.6 \text{ V}$ ; v) continuous scan  $+0.1$  to  $-1.6 \text{ V}$ . Scan rates are  $0.1 \text{ V/s}$  except for v) which is  $10 \text{ V/s}$ . Reproduced with permission from ref. [49].



In the initial negative going scan (from +0.1 V) (Figure 6, b,iii) only this four-electron reduction process is seen. Successive scans however, reveal couples due to the mononuclear MnPc species formed at the electrode surface (see Scheme I in [94]).

Note that formation of the oxo bridge stabilizes Mn(III)Pc, relative to the mononuclear species, by  $\approx 0.75$  V.

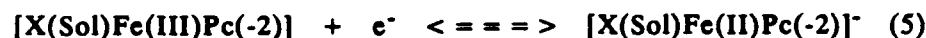
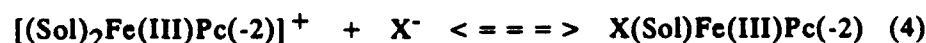
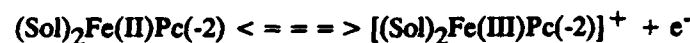
A one-electron oxidation was observed in pyridine at about +0.35 V, presumably to form  $[\text{Pc}(-2)\text{Mn(IV)-O-Mn(III)Pc}(-2)]^+$  but this complex was insufficiently stable to prove its identity spectroscopically [94].

#### iv. Iron, Ruthenium, and Osmium Phthalocyanines

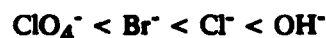
Iron(II) phthalocyanine is fairly soluble in a wide range of donor solvents (and some nondonor solvents), and this solubility, in distinction to species such as OTiPc, OVPC etc., has led to many studies of its electrochemical properties in solution [4, 6, 10, 54, 60-62, 93, 97-102].

Iron(II) phthalocyanine commonly displays four reversible couples in the range +1.00 - (-2.00) V (Table 6). Oxidation to  $[\text{Fe(III)Pc}(-2)]^+$  occurs in the range -0.15 - (+0.69) V highly dependent upon the solvent and counteranion. Iron(II) phthalocyanine binds donor solvents to form six-coordinate  $(\text{Sol})_2\text{Fe(II)Pc}(-2)$  species, while the  $\text{Fe(III)Pc}$  oxidation product has been proven by electronic and electron spin resonance spectroscopy [97].

Thus, analysis of the scan rate dependence of the anodic and cathodic currents (for the oxidation couple) [93, 103] demonstrates a reversible electron transfer followed by a chemical reaction upon oxidation:

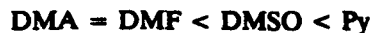


In this case strong binding of the counteranion in  $[X(\text{Sol})\text{Fe(III)Pc}(-2)]^+$  greatly influences the potential at that the  $\text{Fe(III)/Fe(II)}$  process is observed. Reaction (4) must proceed rapidly to the right, but not to the left, relative to the voltammetric time scale, and thus the stability of  $X(\text{Sol})\text{Fe(III)Pc}(-2)$  determines the observed  $\text{Fe(III)/Fe(II)}$  potential, shifting to more negative potentials in the sequence:



Pyridine stabilizes  $\text{Fe(II)Pc}$ , through formation of  $(\text{Py})_2\text{Fe(II)Pc}(-2)$  to such

a degree that the oxidation product,  $[(\text{Py})_2\text{Fe(III)Pc}(-2)]^+$  is unstable in pyridine and there is a marked loss of cathodic current on the return wave. The Fe(III)/Fe(II) couple shifts positively in the sequence:



and linearly follows the Gutmann donor number for the solvent [95].

Thus the most negative potential is obtained by dissolving Fe(II)Pc in DMA or DMF in the presence of chloride ion. Indeed this combination leads to an air sensitive solution that oxidizes directly in air to the Fe(III) species [97].

In contrast to the situation with Mn(II)Pc, the first reduction process with Fe(II)Pc also shows quite strong solvent dependence shifting negatively in the sequence  $\text{DMA} < \text{DMSO} < \text{Py}$  (Table 6), but little dependence upon anion. Electronic and electron spin resonance data clearly show formation of  $[\text{Fe(I)Pc}(-2)]^-$  species. Moreover, the latter experiment, in the presence of pyridine as solvent (or with imidazole/DMA or  $\text{Ph}_3\text{P/DMSO}$ ), clearly identifies a five coordinate  $[\text{LFe(I)Pc}(-2)]^-$  species [97]. Analysis of the scan-rate dependence of the current then confirms a reversible electron transfer followed by a chemical reaction, consistent with (and generalizing for solvent, Sol):



With increasing donor strength of solvent, the  $(\text{Sol})_2\text{Fe(II)Pc}(-2)$  species is stabilized. Since anion binding is not involved, there is little dependence thereon. The sequence of solvent dependence is the reverse of that of the Fe(III)/Fe(II) couple, because it is now the higher, rather than the lower, oxidation state that is being preferentially stabilized.

However, the situation is more complex than this as shown by the variable scan rate data shown in Figure 7. Two pairs of couples associated with the Fe(II)/Fe(I) process can be seen. The data may be explained by consideration of two additional equilibria:



Given that six-coordinate  $[(\text{Sol})_2\text{Fe(I)Pc}(-2)]^-$  would oxidize at a more negative potential (Eq. 6) than five coordinate  $[(\text{Sol})\text{Fe(I)Pc}(-2)]^-$  (Eq. 8) (due to increased destabilization of the filled  $d_{22}$  orbital), then the former equilibrium (6), is associated with couple B,B' (Figure 7) and the latter with A,A'. Reduction of six-coordinate Fe(II)Pc (Eq. 6) leads to rapid loss of solvent (Eq. 7). At slow

scans, on the reverse scan, there is sufficient time for reaction (7) to proceed to the left to a large degree, hence wave B is more prominent than wave A. At high scan rates, there is insufficient time, permitting reaction (8) to dominate, and therefore wave A becomes more intense than wave B. The observation of wave A' at high scan rates demonstrates that equilibrium (9) does not proceed so rapidly to the right [97].

The next reduction process occurs at the phthalocyanine ring, to form  $[(\text{Sol})\text{Fe}(\text{I})\text{Pc}(-3)]^{2-}$ . Since Fe(II) is not involved, this second reduction couple shows little solvent or anion dependence. It varies from the first reduction by some 0.2 (Py) to 0.7 V (DMA). The very small separation for pyridine follows from the strong stabilization of Fe(II)Pc by this solvent. The scan rate/current dependence is consistent with a simple electron transfer without any following chemical reaction, consistent with the assignment. Further reduction, likely to form  $[(\text{Sol})\text{Fe}(\text{I})\text{Pc}(-4)]^{3-}$  occurs at a potential  $\approx 0.6$  V more negative (Table 6).

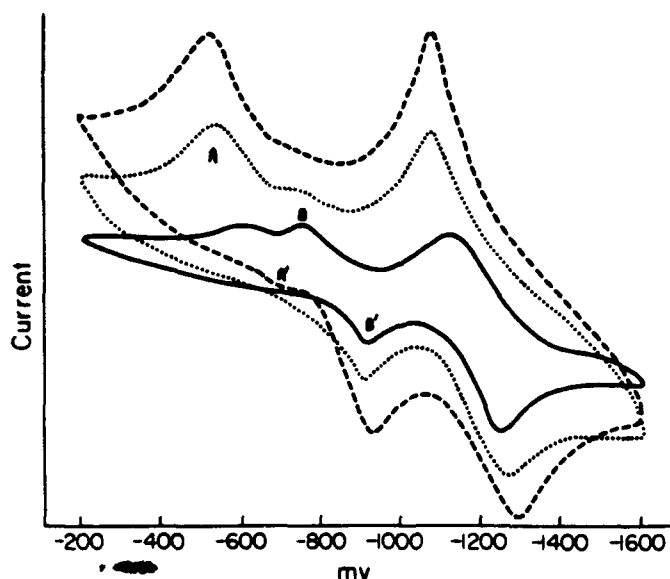


Figure 7 Variable Scan Rate Data for Fe(II)Pc/DMA/TEABr. Scan rates from lower to upper curves are 0.1, 10 and 50 V/s respectively. Wave A does not appear in a voltammogram scanned at 0.01 V/s. Reproduced with permission from Ref. [97].

Kadish, Bottomley, and Cheng [98] have reported a detailed spectroscopic and electrochemical study of  $\text{Fe(II)Pc}$  in the presence of the bases (L) imidazole, 2-methylimidazole, N-methylimidazole, and a range of mono-di- and trisubstituted pyridines. They report binding constants for these ligands, in DMSO, for  $\text{L}_2\text{Fe(II)Pc}(-2)$  ( $\text{Log } K_1$  and  $\text{Log } K_2$ ) and for  $[\text{LFe(I)Pc}(-2)]^-$ , obtained by spectroscopic or electrochemical analysis of ligand-titrated solutions of  $\text{Fe(II)Pc}$  in DMSO, but the reader should note some dissenting arguments in [130].

Figure 8 shows how couple I, (Eqs. 6,7) shifts toward couple II ( $[\text{LFe(I)Pc}(-2)]^-/[\text{LFe(I)Pc}(-3)]^{2-}$ ,  $\text{L} = \text{DMSO}$  or imidazole, depending upon concentration of imidazole) with increasing imidazole concentration and merging therewith at concentrations greater than 0.1 M [Im] (or (N-MeIm)). A plot of  $E_{1/2}$  versus  $\log [\text{L}]$  gave a slope of  $-57 \text{ mV/pH}$  unit consistent with the loss of one ligand upon reduction. The newly formed process (III) is a two-electron reduction forming  $[(\text{Im})\text{Fe(I)Pc}(-3)]^{2-}$  directly from  $(\text{Im})_2\text{Fe(II)Pc}(-2)$ .

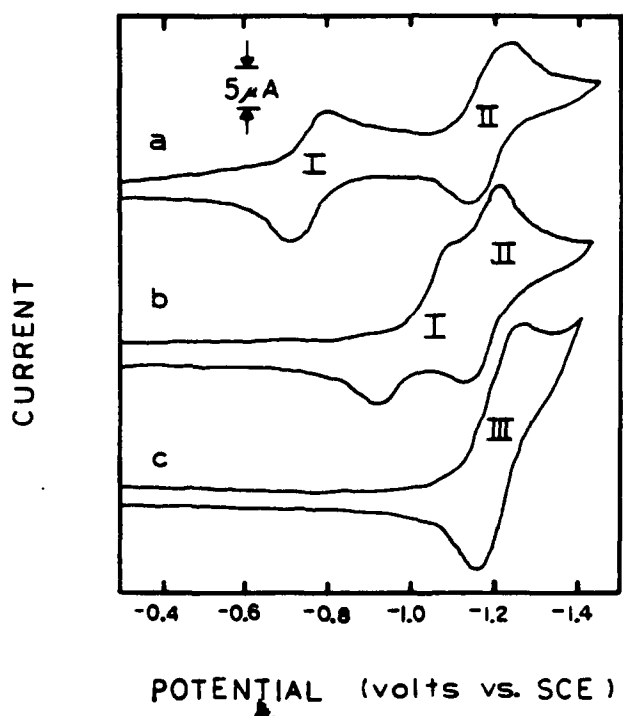


Figure 8 Cyclic voltammetry of iron phthalocyanine (1.18 mM) in  $\text{Me}_2\text{SO/imidazole/0.1 M TEAP}$ . Scan rate 0.1 V/s; Imidazole concentrations, a) 0, b) 0.01 M, c) 0.095 M. Reproduced with permission from Ref. [98].

Careful analysis of the electrochemical data shows that there are two sequential one-electron processes at the same potential (EE process), with the first (corresponding with Eqs. 6, 7) being rate controlling. The addition of imidazole has no effect upon the potential of couple II.

This observation is in contrast to the titration of 2-methylimidazole, 1,2-dimethylimidazole, and a range of different substituted pyridines in DMSO. At low concentrations ( $\log [L] < 0.05$  M) only couple I shifts negatively, and couple II is invariant, but at higher concentrations both couples shift negatively, and with the same slope ( $\approx -57$  mV/pH unit). Thus both the  $L_2Fe(II)Pc(-2)$  and  $[LFe(I)Pc(-2)]^-$  species lose a ligand L upon reduction finally to form  $[(DMSO)Fe(I)Pc(-3)]^{2-}$ . With these ligands, couples I and II do not coalesce.

Finally, data for the sterically hindered ligands 2,4-lutidine or 2,4,6-collidine were interpreted in terms of binding of these ligands to  $Fe(II)Pc(-2)$  but not to  $[Fe(I)Pc(-2)]^-$ .

A very early study [62] reported 0.19 V for the  $Fe(II)Pc$  oxidation couple in the noncoordinating chloronaphthalene. This datum likely then refers to oxidation of the four coordinate  $Fe(II)Pc$  fragment, but whether oxidation occurs at the metal center or phthalocyanine ring was not proven.

While  $Fe(II)Pc$  in common with all other unsubstituted metallophthalocyanines, is insoluble in water, it will dissolve therein, in the presence of cyanide ion, forming the somewhat water-soluble  $[(CN)_2Fe(II)Pc(-2)]^{2-}$  [18a, 86, 100]. Data for this species (Table 6) have been reported by three groups [100, 88, 105]. It shows an  $Fe(III)/Fe(II)$  oxidation wave at 0.14 V (in acetone) (or 0.04 V in  $CH_2Cl_2$ ), indicating rather strong stabilization of the  $Fe(III)$  state by the bound cyanide ligands. The three sets of data, in different solvents, show rather dramatically different potentials that might indicate significant solvatochromism, but the system should be reinvestigated. In acetone [88] the  $Fe(II)/Fe(I)$  couple falls at a very typical potential, suggesting that cyanide does not especially favor binding to  $Fe(II)$ . Curiously, however, the next reduction, forming the  $[Fe(I)Pc(-3)]^-$  anion radical species, is found some 0.1 - 0.3 V more negative than all other observations. Ring oxidation is seen at 0.7 - 1.16 V.

Various ring substituted iron phthalocyanines have been studied. The tetrasulfonated species,  $Fe(II)[TsPc]$  has potentials very closely similar to those of the unsubstituted species. Its ready solubility permitted a detailed spectroelectrochemical study as a function of pH [101]. The aggregation properties of  $Co[TsPc]$  and  $Fe[TsPc]$  were studied as a function of oxidation state and the results have been reported in Table 3 of [101]. In summary:

$M(I)[TsPc(-2)]$  species ( $M = Co, Fe$ ); nonaggregated in acid and base.

$Co(II)[TsPc(-2)]$  species; aggregated in acid and base.

$Fe(II)[TsPc(-2)]$  species; partly aggregated in acid and base.

$Co(III)[TsPc(-2)]$  species; nonaggregated in acid, probably dimeric in base.

$Fe(III)[TsPc(-2)]$  species; aggregated in acid, probably dimeric in base.

These results strictly only apply to the conditions used and, in general, aggregation will diminish with dilution.

The corresponding tetracarboxy species  $\text{Fe(II)[TcPc]}$  is reported [71] to have an oxidation potential of 1.22 V but this is far too positive to be due to  $\text{Fe(III)/Fe(II)}$  and must refer to oxidation of the  $\text{Fe(III)[TcPc]}$  species (Table 6).

The hexadecachlorophthalocyanines have unusual electrochemical properties [63]. The presence of 16 substituting chlorine atoms is expected to greatly stabilize ring reduction and destabilize metal centered oxidation. The former prediction is clearly demonstrated by reduction of  $\text{Zn(II)[Cl}_{16}\text{Pc(-2)]}$  (unequivocally to  $[\text{Zn(II)[Cl}_{16}\text{Pc(-3)}]^-$ ) occurring some 0.3 V or more positive of the usual reduction potential [63] (Table 2). The observed oxidation potential, for  $\text{Fe(II)[Cl}_{16}\text{Pc(-2)]}$  in DMF, at 0.73 V agrees with the latter prediction, being much more positive than most other  $\text{Fe(III)/Fe(II)}$  couples. Reduction yields two waves at -1.11 and -1.73 V but the former cannot be assigned to the  $\text{Fe(II)/Fe(I)}$  couple since it falls considerably negative of this process in all other iron phthalocyanines, rather than positive as expected. Rather these two processes must be assigned to reduction to  $[\text{Fe(I)[Cl}_{16}\text{Pc(-3)}]]^{2-}$  and then to  $[\text{Fe(I)[Cl}_{16}\text{Pc(-4)}]]^{3-}$  occurring at more positive potentials than the corresponding processes in other iron phthalocyanine species (Table 6).

The absence of observation of the  $\text{Fe(II)/Fe(I)}$  process, and of the corresponding  $\text{Co(II)/Co(I)}$  process in  $\text{Co(II)[Cl}_{16}\text{Pc(-2)]}$  (see the following), must arise through kinetic sluggishness. The  $\text{M[Cl}_{16}\text{Pc(-2)]}$   $\text{M} = \text{Fe(II), Co(II)}$ , species behave in a very similar fashion [110].

Ercolani and co-workers [106,111] have explored the electrochemistry of  $\text{Pc(-2)Fe(III)-O-Fe(III)Pc(-2)}$  and  $\text{Pc(-2)Fe(III.5)-N-Fe(III.5)Pc(-2)}$ . These species are discussed in some detail in another chapter in this volume [112] and so will only be summarized here. The data are reported in Table 5 of ref. [112] together with corresponding tetraphenylporphyrin measurements.

On the voltammetric time scale,  $\text{Pc(-2)Fe(III)-O-Fe(III)Pc}$  is shown to undergo one-electron oxidation, at 0.47 V in pyridine, to a mixed-valence  $\text{Fe(III)-O-Fe(IV)}$  species and two successive one-electron reductions (-0.59, -0.95 V) to the mixed-valence  $\text{Fe(III)-O-Fe(II)}$  and then  $\text{Fe(II)-O-Fe(II)}$  species with the integrity of the Fe-O-Fe bridge being maintained. Over longer time periods, however, all these reduced or oxidized species cleave and electrochemical waves corresponding to the mononuclear  $\text{FePc}$  fragments are observed. Given that the  $\text{Fe(III)/Fe(II)}$  couple for  $(\text{Py})_2\text{Fe(II)Pc}$  is observed at 0.66 V (Table 6), the oxo bridge confers some 1.25 V stability to  $\text{Fe(III)}$ .

The nitrido dimer displays an oxidation couple at 0.0 V in pyridine, forming the  $\text{Fe(IV)-N-Fe(IV)}$  species, and three successive reductions (-0.83, -1.02, -1.29 V) show bridge integrity. On a longer time scale the first oxidation and reduction processes yield stable species, in contradistinction to the oxo bridged species, but the second and third reduction processes lead to bridge cleavage. Comparing iso-electronic species, the nitrido bridge confers some 1.3 V stability over the

155

corresponding mixed-valence Fe(III)-O-Fe(IV) species.

Ruthenium(II) phthalocyanines have been explored by James and co-workers [12]. Oxidation appears to occur exclusively at the phthalocyanine ring (Table 2). The first half-wave potentials for all complexes studied [12] lie between 0.7-0.9 V (versus SCE) and depend on the nature of the axial ligand. For bispyridine ruthenium phthalocyanines ( $L_2RuPc(-2)$ ) with substituted pyridines in axial position the value of  $E_{1/2}$  decreases in accordance with increasing electron-donor strength of the coordinated ligand in the sequence  $py > 4Me-py > t-Bu-py$  (0.77, 0.74, and 0.70 V respectively). When the solvent molecules serve as axial ligands in  $PcRuL_2$ , the half-wave potentials show changes depending on the nature of the metal-ligand bond: N-bonded (MeCN) 0.72, O-bonded (DMF) 0.80, and S-bonded (DMSO) 0.89 V. The highest value for the half-wave potential of  $(DMSO)_2RuPc$  could be consistent with  $\pi$ -electron acceptance by the S-bonded sulfoxide. If one molecule of pyridine in  $L_2Ru(II)Pc(-2)$  is replaced by CO the potential is higher, for instance, 0.77 V for  $(Py)_2Ru(II)Pc(-2)$  and 0.91 V for  $(Py)(CO)Ru(II)Pc(-2)$ , due to the acceptor effect of the CO ligand.

Data for osmium phthalocyanines are unavailable.

## v. Cobalt, Rhodium, and Iridium Phthalocyanines

In common with  $Fe(II)Pc$ ,  $Co(II)Pc$  is soluble in a wide range of donor and nondonor solvents and its solution electrochemistry has been studied extensively [6, 10, 11, 49, 63, 66, 67, 70, 71, 88, 95, 101, 107, 113-116].

Such electrochemistry can conveniently be split into two sections, that referring to donor solvents, and that referring to nondonor solvents. A series of reversible couples are observed and may be summarized:

### Donor Solvents

- I
- $Co(III)Pc(0)/Co(III)Pc(-1)$
- II
- $Co(III)Pc(-1)/Co(III)Pc(-2)$
- III
- $Co(III)Pc(-2)/Co(II)Pc(-2)$
- IV
- $Co(II)Pc(-2)/Co(I)Pc(-2)$
- V
- $Co(I)Pc(-2)/Co(I)Pc(-3)$
- VI
- $Co(I)Pc(-3)/Co(I)Pc(-4)$

### Non-donor solvents

- I
- $Co(III)Pc(0)/Co(III)Pc(-1)$
- II'
- $Co(III)Pc(-1)/Co(II)Pc(-1)$
- III'
- $Co(II)Pc(-1)/Co(II)Pc(-2)$
- IV
- $Co(II)Pc(-2)/Co(I)Pc(-2)$
- V
- $Co(I)Pc(-2)/Co(I)Pc(-3)$
- VI
- $Co(I)Pc(-3)/Co(I)Pc(-4)$

(11)

(net charges omitted for clarity), where the principle difference lies in whether, for Co(II)Pc, the metal or the ring is oxidized first. Donor solvents (or coordinating counteranions or other ligands in nondonor solvents) strongly favor Co(III)Pc by coordinating along the axis to form a six-coordinate  $L_2Co(III)Pc$  species. If such donor molecules are absent, then oxidation to Co(III) is inhibited and ring oxidation occurs first. Table 7 summarizes data for CoPc species in nondonor solvents, while Table 8 collects data for CoPc species in the presence of donors (solvents or added ligands) (see also Figure 5) [49].

Cobalt(III) (in common with Fe(II)) has a much stronger propensity to form six-coordinate (low spin,  $t_{2g}^6$ ) species than does Fe(III), or any other first row transition metal M(III) species; thus these observations are characteristic of CoPc. Note that the simple replacement of solvent DCB with solvent DMF shifts the Co(III)/Co(II) potential by some 600 mV although the comparison is not strictly valid since the oxidation occurs within Pc(-1) in DCB and Pc(-2) in DMF.

A range of six-coordinate  $[X_2Co(III)Pc(-2)]^-$  anions has been studied, with variously substituted phthalocyanines, by both the Hanack [88] and Orihashi [71] groups (Table 8); where the same compound has been studied by both groups, there are some rather large discrepancies in oxidation potential due, perhaps, to rather different conditions of measurement.

The products from couples (II) through (V) (11) have all been proved by electronic and/or electron spin resonance spectroscopy and their identity is assured. Couples I and VI are assigned by inference but are likely to be correctly identified.

When Co(II)[TBuPc(-2)] is oxidized at 0.64 V in DCB solution the purple color of the radical cation,  $[Co(II)[TBuPc(-1)]]^+$  is formed, but when pyridine is added the purple color changes immediately to green producing the characteristic spectroscopic features of Co(III) phthalocyanine, viz  $[(Py)_2Co(III)[TBuPc(-2)]]^+$  [117]. This is an equilibrium process, and with relatively low concentrations of pyridine in DCB,  $\sim 10^{-2}$  M, the process is thermally reversible, the cation radical being regenerated at high temperatures. In a similar experiment, the addition of chloride ion also converts the Co(II) cation radical,  $[Co(II)[TBuPc(-1)]]^+$ , to a chloro cobalt(III) species, probably  $[Cl_2Co(III)[TBuPc(-2)]]^-$  [67].

More extreme chemistry occurs if hydroxide ion is added, as will be discussed below. Thus the redox couples of the Co(II)[TNPc(-2)] system do depend critically on whether coordinating anions are present. In studying cobalt phthalocyanine electrochemistry care must be taken to exclude extraneous donors (anions or otherwise) except where their presence is explicitly required.

An earlier study [95] explored the effect of varying the donicity of the solvent on the Co(III)/Co(II) potential. In this case pyridine yields the least positive redox potential and DMSO the most. The Co(III)/Co(II) potential is irreversible in DMA so that a datum for this solvent is not available. Nevertheless the shift to more negative potentials from DMSO to Py is the



Table 7 Electrochemical Data for Mononuclear and Polynuclear Cobalt Phthalocyanines (Non-donor Solvents) (Versus SCE).

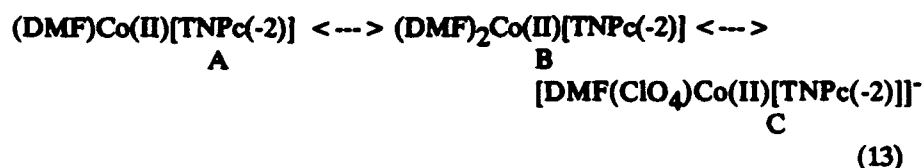
Species	I	II	III	IV <sup>a</sup>	Ring Reduction <sup>b</sup>	Solv.	Ref.
Co(II)Pc			0.77			ClNap	74
Co(II)Pc		1.12	0.61			DCB	10,66,67
Co(II)Pc			-0.64	-1.34 <sup>b</sup>		MeNp/150°	52
Co(II)[TBuPc]				-0.64		MeNp/150°	52
Co(II)[TBuPc]				-0.75		CH <sub>2</sub> Cl <sub>2</sub>	52
Co(II)[TcPc]	1.20					ACN	71
Co(II)[TNPc(-2)]	1.36	1.08	0.52	-0.42	-1.58	DCB	115,47 <sup>c</sup> ,49
Co(II)[TNPc(-2)]		0.98	0.42	-0.52		DCB/TBAPF <sub>6</sub>	115
EtMeO(5)[Co(II)TrNPc] <sub>2</sub>	1.36	(d)	0.54	-0.44	-1.58	DCB	49
Me <sub>2</sub> O(5)[Co(II)TrNPc] <sub>2</sub>		0.55	-0.46	-1.58		DCB	47
Ca(4)[Co(II)TrNPc] <sub>2</sub>	1.38	(d)	0.52	-0.44	-1.58	DCB	49
C(2)[Co(II)TrNPc] <sub>2</sub>	1.36	0.82	0.52	-0.45	-1.58	DCB	49
O(1)[Co(II)TrNPc] <sub>2</sub>	1.40	1.00	0.53	-0.44	-1.58	DCB	49
(-1)[Co(II)TrNPc] <sub>2</sub>		1.08	0.66	-0.32	-1.20, -1.47 <sup>c</sup>	DCB	119
[Co(II)TrNPc]	1.35	0.99	0.54	-0.43	-1.57	DCB	114
Co(II)[TsPc]		0.77	0.19			ClNap	95

<sup>a</sup> Processes: I, Co(III)Pc(0)/Co(III)Pc(-1); II, Co(III)Pc(-1)/Co(II)Pc(-1); III, Co(II)Pc(-1)/Co(II)Pc(-2); IV, Co(II)Pc(-2)/Co(I)Pc(-2). Some waves show some splitting due to the stabilisation of mixed valence species, but these were ill-defined. <sup>b</sup> Reduction processes of Co(I)Pc(-2). <sup>c</sup> The [Co(II)[TNPc(-1)]<sup>+</sup>/Co(II)[TNPc(-2)] datum reported in [47] appears anomalous. <sup>d</sup> Not resolved. <sup>e</sup> Mixed valence splitting? Note that some data collected versus an internal ferrocene couple reference are corrected according to Table 1.

reverse of the sequence observed for the oxidation of Fe(II)Pc because it is now the higher oxidation state, Co(III), that is being stabilized by the more strongly donor solvents, rather than the lower, as is the case for Fe(II)Pc. A series of substituted pyridines [95] show potentials for both Co(III)/Co(II) and Co(II)/Co(I) shifting to more negative potentials with increasing base strength ( $pK_a$ ). It is not uncommon for the Co(III)/Co(II) couple to be irreversible because of the large change in spin state, and the likely change in Co-L bond length during this redox process.

Both Fe(II)Pc and Co(II)Pc show M(II)/M(I) potentials that linearly follow the Gutmann donor number with the same sign of the slope since now it is both Co(II) and Fe(II) that are stabilized by the stronger donor solvent [95]. However, nondonor solvents do not fall on the same line [95] as donor solvents, that is, they do not behave simply as very weakly donor solvents. This is a consequence of the fact that in donor solvents the Co(II)Pc will be solvated (five or six-coordinate) while in nondonor solvents it will be unsolvated (four coordinate, different spin state).

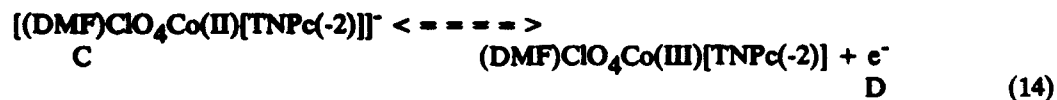
A more detailed study of the electrochemistry of Co(II)Pc in DMF reveals more subtle features [49]. A solution of Co(II)[TNPc(-2)] in DMF/ $ClO_4^-$  contains several species in equilibrium, viz:



which will have three different Co(III)/Co(II) oxidation potentials.

However, if the equilibria are facile only the oxidation of the most easily oxidized species, which should be C, should be observable. It appears however, that both the  $[Co(III)[TNPc(-2)]]^+ / Co(II)[TNPc(-2)]$  and  $[Co(III)[TNPc(-1)]]^{2+} / [Co(III)[TNPc(-2)]]^+$  redox couples are coupled to other equilibria that are relatively slow on the voltammetric time scale and can be probed by variable-scan-rate studies.

The  $[Co(III)Pc(-2)]^+ / Co(II)Pc(-2)$  process (labelled IIIa), (IIIc) in Figure 9) has a scan-rate-dependent  $i_c/i_a$  ratio approaching unity at higher scan rates and higher perchlorate ion concentrations. This is interpreted in terms of the following processes [49]





Equilibrium (15), which is suppressed in excess perchlorate ion, produces five coordinate species E, which is expected to be much easier to reduce than species D, that is, the Co(III)/Co(II) couple of E will occur at more positive potentials. Thus C is oxidized to D, at (IIIa) (Figure 9). D rearranges to E, at least to a small degree, and E is spontaneously reduced on the positive side of (IIIa) since its reduction potential lies positive of (IIIa). Equilibrium (15) is driven to the right by this reduction process and therefore decreases the intensity of the current at (IIIc). At higher scan rates, there is less time for the rearrangement to occur and more reversible behavior obtains.

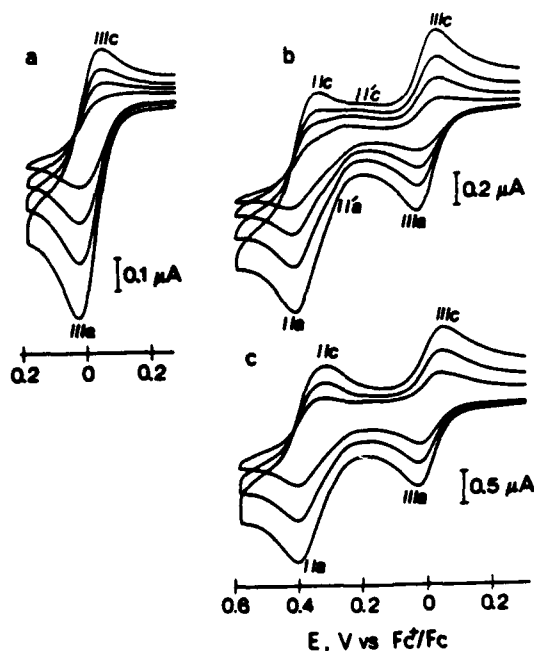


Figure 9 Cyclic Voltammetry of Co(II)[TNPC(-2)] ( $1 \times 10^{-4}$  M) in DMF/(0.3 M TBAP), at varying scan rates and switching potentials. a) Co(III)/Co(II) couple at 2, 5, 10 and 20 mV/s; b) Pc(-1)/Pc(-2) and Co(III)/Co(II) couples at 2, 5, 10 and 20 mV/s; c) as (b), at 20, 50 and 100 mV/s. Reproduced with permission from Ref. [49].

Table 8 Electrochemical Data for Mononuclear and Polynuclear Cobalt Phthalocyanines<sup>a</sup> (Donor solvents) (Versus SCE)

Species	I	II	III	IV <sup>a</sup>	Reduct. Proc. <sup>b</sup>	Solvent	Ref.
Co(II)Pc	1.15	0.21	-0.55	-0.91	-1.44	Py	61,107
Co(II)Pc		0.80	-0.20			DMA	60
Co(II)Pc			-0.37	-1.40	-1.80, -2.08, -2.46	DMF	4
Co(II)[TEtPc]	0.94	0.49	-0.32	-1.45		DMF	131 <sup>c</sup>
Co(II)[TBuPc]			-0.75			DMSO	52
Co(II)[TcPc]			-0.28	-0.42?		H <sub>2</sub> SO <sub>4</sub>	116
Co(II)[TcPc]	1.20					ACN	120
Co(II)[TNPc(-2)]	0.78	0.38	-0.45	-1.59		DMF	49
Co(II)[TNPc(-2)]	1.14	0.43	-0.63			DCB/Cl	115
Co(II)[Cl <sub>16</sub> Pc]		1.09	(d)	-1.21	-1.69	DMF	63
Co(II)[TsPc]		0.04	-0.71			Py	95
Co(II)[TsPc]		0.01	-0.725			4-EtPy	95
Co(II)[TsPc]			-0.85qr	-1.35qr		H <sub>2</sub> O	64
Co(II)[TsPc]		0.46	-0.60			DMSO	95
Co(II)[TsPc]		0.43irr	-0.50			DMF	95
Co(II)[TsPc]		0.16	-0.64			3-ClPy	95
Co(II)[TAPc]	0.7,0.5 <sup>e</sup>	0.17	-0.52	-1.66		DMSO	70
Co(II)[TAPc]	0.60 <sup>e</sup>	0.16	-0.52	-1.74		DMF	132 <sup>c</sup>
Co(II)[TAPc]	0.68					ACN	120
Co(II)[TNO2Pc]	1.26					ACN	120
Co(II)[TMzPc]	0.69					ACN	120
Co(II)[OCNPc]	1.76					ACN	120
Co(II)[OCPC]	1.61					ACN	128

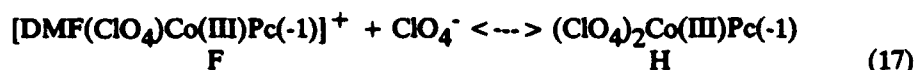
Species	I	II	III	IV <sup>a</sup>	Reduct. Proc. <sup>b</sup>	Solvent	Ref.
Co(II)[OMePc]	0.74					ACN	128
Co(II)[OMPc]	0.79					ACN	120
Na[(CN) <sub>2</sub> Co(III)[TAPc]]		0.20 <sup>c</sup>	-0.55 <sup>f</sup>	-1.15		DMF	132 <sup>c</sup>
K[(CN) <sub>2</sub> Co(III)[TAPc]]	0.55					ACN	71
Na[(CN) <sub>2</sub> Co(III)[TEAPc]]	0.87		-0.43	-1.48		DMF	131 <sup>c</sup>
Na[(CN) <sub>2</sub> Co(III)Pc]	0.62		-0.94 <sup>f</sup>	-1.52		Acetone	88
K[(CN) <sub>2</sub> Co(III)Pc]	0.88		-0.91 <sup>f</sup>	-1.54		Acetone	88,121
K[(CN) <sub>2</sub> Co(III)Pc]	1.06					ACN	71
Bu <sub>4</sub> N[(SCN) <sub>2</sub> Co(III)Pc]	0.88	-0.34	-1.02	-1.52		Acetone	88
K[(SCN) <sub>2</sub> Co(III)Pc]	0.94					ACN	71
K[(SCN) <sub>2</sub> Co(III)Pc]	0.84	-0.32	-0.95	-1.49		Acetone	88
Na[(CN) <sub>2</sub> Co(III)[OMPc]]	0.92		-0.83 <sup>f</sup>	-1.46		Acetone	88
K[(CN) <sub>2</sub> Co(III)[OMPc]]	0.59					ACN	71
Na[(CN) <sub>2</sub> Co(III)[OMPc]]	0.61					ACN	71
Na[(CN) <sub>2</sub> Co(III)[TBuPc]]	0.77		-0.93 <sup>f</sup>	-1.50		Acetone	88
Na[(CN) <sub>2</sub> Co(III)[NO <sub>2</sub> Pc]]	1.30 <sup>g</sup>		-0.48 <sup>f</sup>	-1.13		Acetone	88
[(CN)Co(III)[TEAPc]] <sub>n</sub>	0.91		-0.40	-1.49		DMF	131 <sup>c</sup>
[(CN)Co(III)[TAPc]] <sub>n</sub>		0.16 <sup>h</sup>	-0.60 <sup>f</sup>	-1.82		DMF	132 <sup>c</sup>

<sup>a</sup> Processes: I, Co(III)Pc(-1)/Co(III)Pc(-2); II, Co(III)Pc(-2)/Co(II)Pc(-2); III, Co(II)Pc(-2)/Co(I)Pc(-2). Polynuclear species shown in this Table do not display mixed valence behavior. <sup>b</sup> Further reduction processes of Co(I)Pc(-2). <sup>c</sup> Authors of [131,132] correct their ferrocene internal data to SCE using 0.49 V vs SCE. <sup>d</sup> Not observed, probably because of kinetic sluggishness. <sup>e</sup> Irreversible. <sup>f</sup> 2-Electron combined Co(III) → Co(II) → Co(I). <sup>g</sup> Close to solvent limit. <sup>h</sup> Polymetric species oxidation.

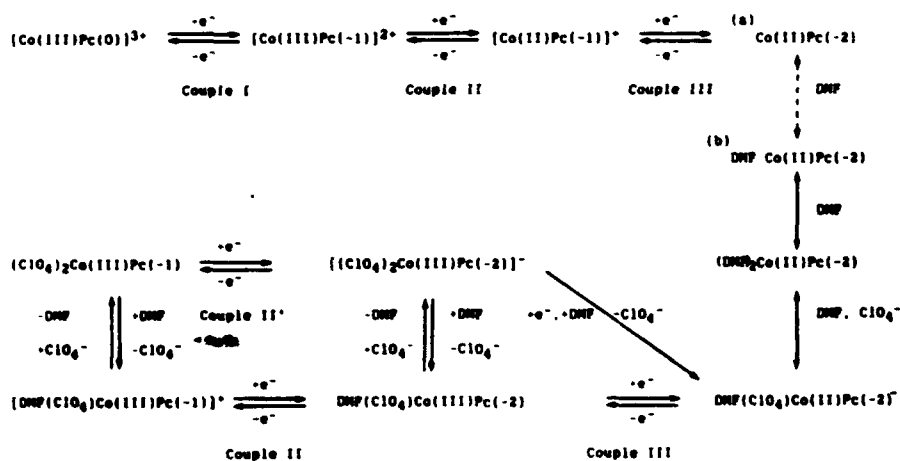
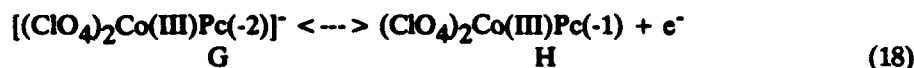
Note that evidence for the kinetic lability of six-coordinate Co(III) macrocycles has been presented [118]. Now, considering the  $[\text{Co(III)Pc(-1)}]^{2+}/[\text{Co(III)Pc(-2)}]^+$  process (labeled (II) in Figure 9), two different pairs of couples, II and II', are observed. With increasing scan rate the more positive couple, IIc grows at the expense of the less positive wave IIc', and vice versa. Moreover increasing perchlorate ion concentration favors wave II'. Therefore wave IIc' must be associated with additional bound perchlorate ion and is then reasonably associated with  $(\text{ClO}_4)_2\text{Co(III)Pc(-1)}$

These processes are understood in terms of the following equilibria:

Process II



Process II'



Scheme I

At slow scan rates, scanning positively from couple III, we initially observe oxidation  $D \rightarrow F$  at IIa. This rearranges via (17) to give mainly H which is reduced at II'c. At higher scan rates, there is insufficient time for equilibrium (17) to occur and reduction of species F is observed at IIc. Wave II'a is never obvious because species G never has the opportunity to build up (see Scheme I) [49].

In summary, couples (14), (16) and (18) are observed, in DMF, at +0.38V, +0.78 and +0.70 V, versus SCE, the data having been corrected, using Table 1, from the original experimental data internally referenced to the ferricenium/ferrocene couple.

A spectroelectrochemical study of  $\text{Co(II)[TsPc(-2)]}$  [101] as a function of pH reveals (Table 7) the varying degrees of aggregation of this species as a function of oxidation state. Unlike  $\text{Fe(II)TsPc}$ , reduced  $\text{M(I)TsPc}$  species are nonaggregated, but higher oxidation state  $\text{Co(III)}$  species are less aggregated than  $\text{Fe(II)}$  species. This is attributed to the dominant formation of six-coordinate  $\text{Co(III)}$  species where the axial groups inhibit aggregation.

When hydroxide ion is added to a DMF (or DCB) solution of  $\text{Co(II)[TNPc(-2)]}$ , under nitrogen, the solution is converted, within the time of mixing, into a 1:1 mixture of  $[\text{Co(I)[TNPc(-2)]}]^-$  and  $[(\text{OH})_2\text{Co(III)[TNPc(-2)]}]^-$ . Thus  $\text{Co(II)[TNPc(-2)]}$  cannot exist in a DMF (or DCB) solution containing hydroxide ion. Naturally, if air is introduced, there is total conversion to the  $[(\text{OH})_2\text{Co(III)[TNPc(-2)]}]^-$  species [11]. Some interesting electrochemical observations arise in this system whose voltammetry is shown in Figure 10 (Left).

If a disproportionated solution of  $\text{Co[TNPc(-2)]}$  in  $\text{DMF/OH}^-$  is oxidized at a potential  $\sim 200$  mV positive of couple A (Figure 10 (Left)) then oxidation totally to  $[(\text{OH})_2\text{Co(III)[TNPc(-2)]}]^-$  occurs. If the solution is polarized  $\sim 200$  mV negative of couple A, then the solution is totally converted to  $[\text{Co(I)[TNPc(-2)]}]^-$ ; in neither case is any intermediate  $\text{Co(II)[TNPc(-2)]}$  observed.

Couple A has the electrochemical characteristics of a one-electron process having the same current intensity as observed in the absence of hydroxide ion [see Figure 10 (Left) a,b,c] yet clearly a two-electron process occurs when the electrode is polarized at this potential.

To understand this observation, a series of experiments was undertaken. If DMF solutions of  $\text{Co(II)[TNPc(-2)]}$  are treated with hydroxide ion and left under nitrogen for an hour or so, all the  $[(\text{OH})_2\text{Co(III)[TNPc(-2)]}]^-$  is reduced to  $[\text{Co(I)[TNPc(-2)]}]^-$ . Such solutions of pure  $[\text{Co(I)[TNPc(-2)]}]^-$  do not display couple B because  $\text{Co(II)[TNPc(-2)]}$  is never formed in these solutions.

Initially, prior to addition of hydroxide ion, we may consider two processes, A,B [Figure 10 (Left) a)] that are associated with  $\text{Co(II)/Co(I)}$  and  $\text{Co(III)/Co(II)}$  respectively, both showing one-electron reversible behavior.

Voltammetry was explored in concert with the electronic spectroscopy (Figure 10 (Right)), using fresh deaerated solutions containing, necessarily, a

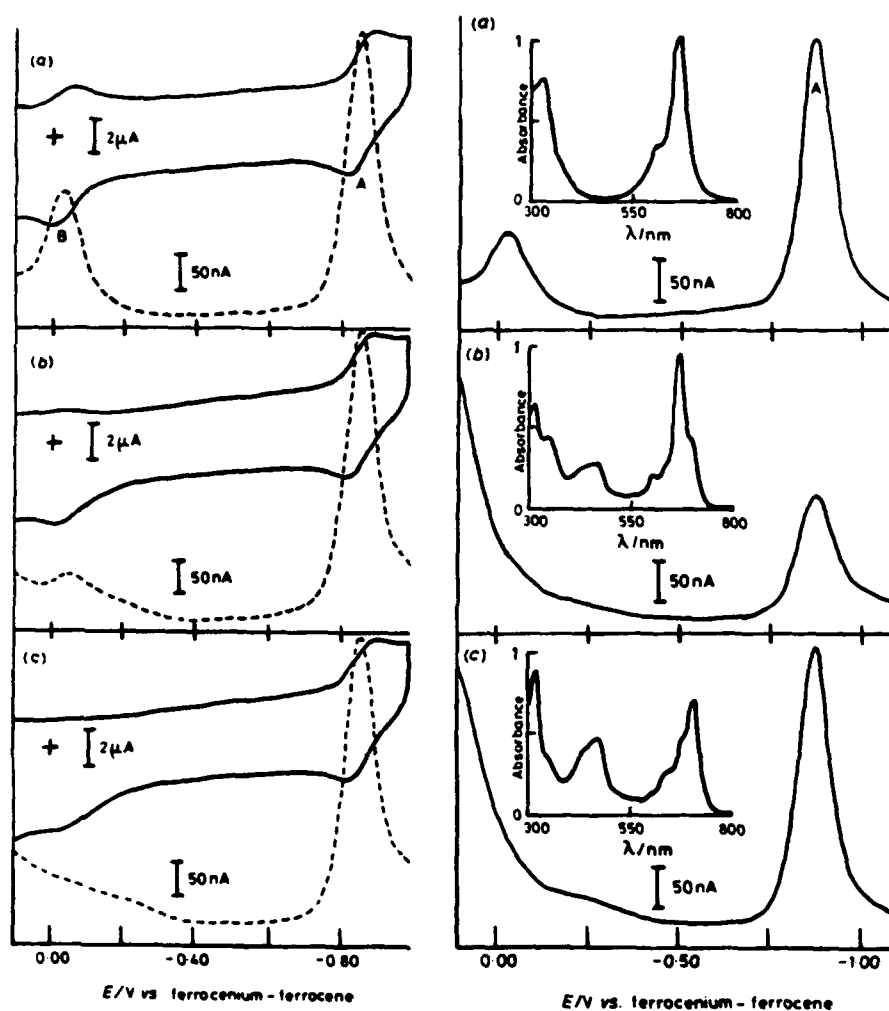


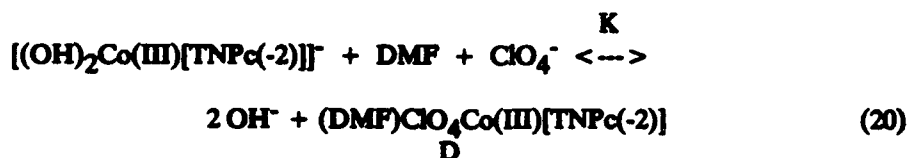
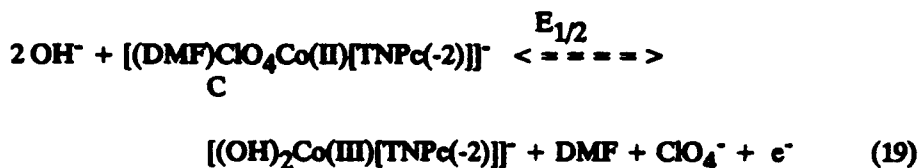
Figure 10 (Left): Cyclic voltammetry (solid line) and differential pulse voltammetry (hatched line) for Co(II)[TNPc(-2)] ( $9.69 \times 10^{-5} \text{ mol dm}^{-3}$ ) at a glassy carbon electrode in DMF/LiOH under nitrogen. Concentration of LiOH; a) 0, b)  $1.4 \times 10^{-4}$ , c)  $2.8 \times 10^{-4} \text{ mol dm}^{-3}$ . B, Right: Electronic spectra and differential pulse voltammetry of Co(II)[TNPc(-2)] ( $1.01 \times 10^{-4} \text{ mol dm}^{-3}$ ) under oxygen. The hydroxide concentrations (NBu<sub>4</sub>OH-MeOH) are a) 0, b)  $5.0 \times 10^{-4}$  (recorded 30 min after mixing), and c)  $5.0 \times 10^{-4} \text{ mol dm}^{-3}$  (recorded 2.5 h later). Reproduced with permission from Ref. [11].



mixture of  $[(\text{OH})_2\text{Co(III)}[\text{TNPC}(-2)]]^-$  and  $[\text{Co(I)}[\text{TNPC}(-2)]]^-$ . One then did not observe (Figure 10 (Right)) couple B  $[\text{Co(III)}/\text{Co(II)}]$  while the current intensity for couple A  $[\text{Co(II)}/\text{Co(I)}]$  was proportional to the content of  $[\text{Co(I)}[\text{TNPC}(-2)]]^-$ . It was possible to conclude that a pure solution of  $[(\text{OH})_2\text{Co(III)}[\text{TNPC}(-2)]]^-$  would not exhibit couple A. Since it is possible to obtain a pure solution of  $[(\text{OH})_2\text{Co(III)}[\text{TNPC}(-2)]]^-$  by oxygenating the  $[\text{Co(I)}[\text{TNPC}(-2)]]^-$  species in DMF/ $\text{OH}^-$ , one might be curious as to why such a solution was not directly studied. In fact, couple A lies at too negative a potential to be observed in an oxygenated solution, and if the solution is first deoxygenated, fairly rapid reduction to  $[\text{Co(I)}[\text{TNPC}(-2)]]^-$  takes place. These reactions were interpreted in terms of a model where neither  $\text{Co(II)}[\text{TNPC}(-2)]$  nor  $[\text{Co(I)}[\text{TNPC}(-2)]]^-$  react with hydroxide ion but where there is a very strong stabilization of  $\text{Co(III)}[\text{TNPC}(-2)]$  by binding to hydroxide ion. Thus the potential of couple A should not be affected by hydroxide ion concentration as observed.

The  $\text{Co(III)}/\text{Co(II)}$  couple, B, upon addition of hydroxide ion to the system, became irreversible, losing its cathodic component (Figure 10 (Right) b)) before it essentially disappeared (Figure 10 (Right) c)). This process corresponds to equilibrium (14), species C,D. In the presence of hydroxide ion, species D forms the dihydroxide and is no longer reducible in the region of couple B so the cathodic component disappears.

The following two processes are now relevant:



and using the electrochemical data to estimate K, the potential for process (19) can be estimated from:

$$E_{1/2}(19) = E_{1/2}(16) - RT/nF[\text{Ln}(K) - 2 \text{ Ln}(\text{OH})]$$

from which [11]:

$$E_{1/2}(19) - E_{1/2}(16) = -0.059[\text{Log}(K) - 2 \text{ Log}(\text{OH})] \quad (21)$$

(where it is assumed that the diffusion coefficients of the initial and final redox products are the same, and where the negative sign to the immediate right of the equality differs from [11] because the redox processes have been defined in the opposite sense here).

To explain the observed behavior, the value of  $E_{1/2}(19)$  must place this couple negative of couple A. Thus the right-hand side of Eq. (21) must be at least 0.9 V. Given also that even micromolar concentrations of  $[OH^-]$  caused a loss of couple B and shifted the Co(III)/Co(II) couple negative of couple A, it was shown that the maximum possible value of  $K(20)$  was  $\sim 10^{-23}$  [11], a not unreasonable value given the evident strong HO-Co(III) binding.

One more observation needed explanation, namely, why does couple A look like a one-electron process, yet, in reality, two-electrons are consumed? Consider using a bulk  $[Co(I)[TNPc(-2)]]^-$  solution and running a cyclic voltammogram approaching couple A from negative thereof. At couple A,  $[Co(I)[TNPc(-2)]]^-$  undergoes a one-electron oxidation to  $Co(II)[TNPc(-2)]$ . Hydroxide ion is not bound to the cobalt center; so this species does not directly oxidize to  $Co(III)Pc$ , but in a following reaction it does disproportionate to form  $Co(I) + Co(III)$ . The potential for this process will be the same as for a hydroxide-free environment so long as this disproportionation process is slow on the voltammetric time scale. Indeed disproportionation is slow (minutes) at low OH:CoPc ratios ( $\sim 5 - 20:1$ ). It is also possible that disproportionation is inhibited at the electrode surface for mechanistic reasons, and does not occur until the  $Co(II)[TNPc(-2)]$  diffuses away [11].

A series of binuclear and tetranuclear cobalt phthalocyanines have been studied [11, 13, 114, 119, 123]. Those whose electrochemical data are reported in Table 7, show no electrochemical evidence for any significant electronic interaction between the two (or more) phthalocyanine units in the molecule exhibiting electrochemical potentials at values closely similar to those of the mononuclear  $Co[TNPc(-2)]$  under similar conditions. They do show some spectroscopic evidence for coupling, but it is evident that such coupling is not large enough to effect the electrochemistry. These species also disproportionate in the presence of hydroxide ion, in an intramolecular sense, forming  $[Co(I)]_2$  and  $[Co(III)]_2$  but not  $[Co(I)Co(III)]$  [11]. Another group of binuclear CoPc species, discussed in Section E, viii do exhibit mixed-valence behavior.

Electron withdrawing substituents on the phthalocyanine ring obviously render the ring more difficult to oxidize and easier to reduce, and vice versa for electron-donating substituents (see Section E, ix).

Some data are available [4,107] for the further reduction of  $[Co(I)Pc(-2)]^-$  as far down as the  $Pc(-5)$  species (Tables 7,8), but this region has not been definitively explored.

Some solution data have been reported for Rh(III) phthalocyanines [108, 109]. Oxidation near 0.9 V yields a Rh(III) radical cation species whose photochemistry has been explored [108].

Chlororhodium phthalocyanine, in DMF or DCB, shows an irreversible reduction wave near -0.7 V that has a cathodic but no anodic component [109]. At this potential, there is reduction to monomeric Rh(II)Pc but this rapidly dimerizes at room temperature in solution yielding a dimeric product that is not re-oxidized until about -0.15 V (in DCB/TBAP, [109]). At about -60°C the dimerization reaction is inhibited and a reversible  $\text{XRh(III)[TNPc(-2)]/Rh(II)[TNPc(-2)]}$  couple is observed. Further reduction of the bulk solution exhibits a reversible wave at -1.47 V that probably forms a monomeric  $[\text{Rh(I)Pc(-2)}]^-$  species although a  $[\text{Rh(II)Pc(-3)}]^-$  species is also possible. Final details of the solution electrochemistry of the dimeric  $[\text{Rh(II)Pc}]_2$  species await clarification [109].

No solution data appear available for iridium phthalocyanines.

## vi. Silver and Gold Phthalocyanines

Copper phthalocyanine was discussed in Section D, ii, and gold phthalocyanine, while known, has not been studied electrochemically.

Silver tetraeneopentoxypthalocyanine has been the subject of intensive electrochemical study [48]. In common with many other metallophthalocyanines,  $\text{Ag(II)[TNPc(-2)]}$  is quite strongly aggregated in solution and the aggregation-disaggregation equilibrium is slow on the voltammetry time scale. Conventional CV or DPV yields a broad wave near 0.6 V attributable, on the basis of spectroelectrochemistry, to oxidation to  $[\text{Ag(III)[TNPc(-2)}]]^+$ . A Nernstian analysis of the data shows that the true half-wave potential for oxidation lies at 0.71 V versus SCE, in DCB. Further oxidation yields  $[\text{Ag(III)[TNPc(-1)}]]^{2+}$  (reversible process) and  $[\text{Ag(III)[TNPc(0)}]]^{3+}$  (irreversible process). The possibility that a  $\text{Ag(IV)[TNPc(-2)]}$  species is formed cannot be ruled out. The irreversibility of the third oxidation process may reflect solvent oxidation.

There are two reduction processes which are believed to form  $[\text{Ag(I)[TNPc(-2)}]]^-$  and, probably,  $[\text{Ag(I)[TNPc(-3)}]]^{2-}$ . However, in parallel with the corresponding chemistry of silver(II) porphyrins [133, 134] the silver(I) species are unstable and hydrolyze to form the metal free species at a rate comparable to the electrochemistry time scale. Thus, upon reduction of  $\text{Ag(II)[TNPc(-2)]}$  one observes a pair of waves due to the successive reduction of  $\text{Ag(II)[TNPc(-2)]}$  and a pair of waves due to the successive reduction of the resulting  $\text{H}_2\text{TNPc(-2)}$ . The relative intensities of these pairs of waves are affected both by scan rate and temperature, with higher scan rates and lower temperatures favoring observation of the silver reduction couples.

A more detailed consideration of the relative currents of the reduced species suggested that there was an intermediate between the reduction to  $[\text{Ag(I)[TNPc(-2)}]]^-$  and the formation of reduced  $\text{H}_2\text{TNPc(-2)}$ . This was

postulated to be a sitting-atop version of the  $[Ag(I)[TNPc(-2)]]^-$  species being formed prior to hydrolysis, that is, the large silver(I) sits atop the phthalocyanine ring. Further evidence arises from the fact that even at lower temperatures and higher scan rates, where hydrolysis is largely suppressed, the first reduction couple is irreversible in always showing a larger cathodic than anodic current. A "simple"  $Ag(II)/Ag(I)$  couple, if the  $Ag(I)$  remained in the ring, would be expected to be reversible.

### vii. Polynuclear Phthalocyanines

In addition to the polynuclear metallophthalocyanines and bridged species such as  $PcM-X-MPc$  ( $X = O, N$  etc.), mentioned previously, other bridged species such as  $PcM-LL-MPc$  and  $(-LLMPc-LL-Mpc)_n$  [125] (where  $LL$  is a bridging bifunctional ligand such as pyrazine) are known. However, solution data are not available for the last mentioned species.

Some species, such as the binuclear  $EtMeO(6)[MTrNPc(-2)]_2$  [65] and the tetranuclear spiro linked  $[MTrNPc(-2)]_4$  [65, 114] show no mixed-valence behavior with cobalt(II) (Table 7) but do with Zn(II) (Table 9). Such differences may arise through the presence or absence of axial ligands, respectively inhibiting or facilitating the close approach of phthalocyanine rings.

### viii. Mixed Valence Behavior

Cobalt phthalocyanine complexes of binuclear or tetranuclear phthalocyanines having flexible bridging units, do not exhibit any measureable electrochemical interaction between cobalt centers, that is, mixed-valence behavior is not observed. Rigid systems such as the anthracene and naphthalene bridged binuclear species [126] and the so-called (-1)bridge species [119] do, however, exhibit additional redox waves associated with mixed-valence species (Figure 11). These may be of the metal-centered type, such as  $[Co(II)Pc(-2)]_2/[Co(I)Pc(-2).Co(II)Pc(-2)]^-$  or of the ring-centered type, such as  $[Co(II)Pc(-1)]_2^{2+}/[Co(II)Pc(-1).Co(II)Pc(-2)]^+$ . The splitting of a given redox process due to formation of a stable mixed-valence intermediate, is a measure of the equilibrium (comproportionation) constant,  $K_c$ , for a reaction such as:  $-[M(II)Pc(-1)]_2 + [M(II)Pc(-2)]_2 \rightleftharpoons 2 [M(II)Pc(-1).M(II)Pc(-2)]$  (22) where the mixed-valence splitting,  $\Delta E$  is related to  $K_c$  via:

$$\Delta E = (RT/nF) \ln(K_c) \quad (23)$$

The values of  $K_c$  so obtained for a series of mixed-valence phthalocyanine complexes of cobalt, zinc, aluminum, iron, and silicon are collected in Table 10.

They are seen to range from 20 to  $3 \times 10^8$  (-8 to -49 kJ/mol), thereby showing a wide range of stability. The least strongly coupled systems include some zinc complexes of binuclear phthalocyanines with flexible bridging links where the cobalt analogues do not, in fact, exhibit mixed-valence behavior at all. The rigid bridged systems such as the anthracene, naphthalene and (-1)bridge species exhibit a range of mixed-valence complexes for both zinc and cobalt (Table 10), although in this last case, (-1)bridge, for cobalt, the waves were not well resolved and  $K_c$  values could not be accurately defined.

Generally speaking, mixed-valence species, for a given phthalocyanine, involving the metal ion, such as Co(II)/Co(I) and Co(III)/Co(II) were more stable than those involving the ring Pc(-2)/Pc(-1), and Co(II)/Co(I) species were more stable than Co(III)/Co(II) species.

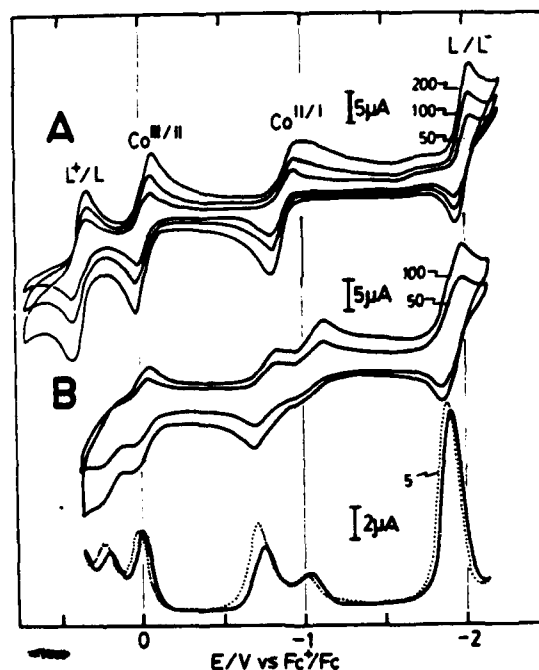


Figure 11 Cyclic and differential pulse voltammograms of (A)  $Co(II)[TNPc(-2)]$  and (B)  $Ant[CoTrNPc]_2$  in DMF at a Pt electrode. Numbers indicated are scan rates. In the differential pulse studies, the solid and dotted lines indicate negative going and positive going scans respectively. Reproduced with permission from Ref. [126].

However, the strongest mixed-valence interactions were seen in ring mixed-valence RSiPc-O-PcSiR species; these exhibit both mixed-valence ring oxidation and mixed-valence ring reduction. The large  $K_c$  values for these silicon species probably reflect the shorter Pc..Pc contacts ( $\approx 3.3 \text{ \AA}$ ) than in the bridged species ( $\approx 4.3 \text{ \AA}$ ). Oligomeric SiPc species have been prepared (Table 3) in that 2, 3 or 4 (or more) OSiPc units are strung together. The mixed-valence species of successively oligomerized species show declining stability of a given mixed-valence species with increasing chain length (Table 3), at least according to Eq.(23). However, it is probable that, due to interaction processes along the chain, this simple equation is inappropriate.

Further, the greater coupling for the Co(II)/Co(I) systems versus the Co(III)/Co(II) likely reflects interaction between the  $d_{z^2}$  orbitals of each cobalt atom, directed along the inter-ring axis, there being an odd  $d_{z^2}$  electron in the Co(I) species. In summary, mixed-valence behavior has been observed for the following binuclear MPc systems:

Pc(-2).Pc(-3) is observed in strongly coupled silicon oligomers, but has not been unequivocally observed with the other bridged binuclear species. The presence of an extra  $\pi$  electron repels the  $\pi$ -electron density in the other ring and therefore inhibits formation of these species unless they are constrained to lie close together.

Pc(-1).Pc(-2) observed with cobalt and with main group ions such as aluminum, zinc and silicon. In the case of cobalt, it is likely that both Co(II) and Co(III) mixed-valence species can be obtained by controlling the solvent (that is, availability of axial ligands). Strong coupling originates in the hole in the  $\pi$  orbital of one ring being capable of delocalization over the other ring.

Co(II).Co(I) is observed in inflexible binuclear species and has electronic spectroscopic characteristics, and  $K_c$  values, consistent with strong coupling between the cobalt centers (along the  $d_{z^2}$  bond axis).

M(III).M(II) is observed in inflexible binuclear species linked through the phthalocyanine rings, or in PcM-O-MPc systems linked through the metal atom, especially for iron.

M(IV).M(III) is observed in PcFe-X-FePc bridged systems, X = O, N.

Some data for mixed valence phthalocyanines containing simple bridges, such as cyanide, oxide or nitride between MPc centers [111, 127, 128] are reported in Table 10. The  $K_c$  values, for M(III)/M(II) systems are comparable with the phthalocyanine bridged systems.

The stability of the "PcFe(IV)-N-Fe(III)Pc" is extraordinary with an electrochemical splitting of 0.83 V corresponding with  $K_c = 1.2 \times 10^{14}$ . The "TPPFe(IV)-N-Fe(III)TPP" analogue is similarly stable (splitting 0.79 V in pyridine [111] or 1.36 V (!) in dichloroethane [129]), likely indicating that these species should best be regarded as class III fully delocalized complexes.

Table 9 Polynuclear Phthalocyanines showing Mixed Valence Behavior

Species	$E_{1/2}^V$ DCB	$E_{1/2}^V$ DMF
<u>EtMeO(5)[Zn(II)TrNPc]<sub>2</sub> [65]</u>		
[Zn(II)Pc(0)] <sub>2</sub> /[Zn(II)Pc(-1)] <sub>2</sub>		1.00
[Zn(II)Pc(-1)] <sub>2</sub> /[Zn(II)Pc(-1).Zn(II)Pc(-2)]	0.49	0.58
[Zn(II)Pc(-1).Zn(II)Pc(-2)]/[Zn(II)Pc(-2)] <sub>2</sub>	0.41	0.43
[Zn(II)Pc(-2)] <sub>2</sub> /[Zn(II)Pc(-3)] <sub>2</sub>	-1.19	-1.04
[Zn(II)Pc(-3)] <sub>2</sub> /[Zn(II)Pc(-4)] <sub>2</sub>	-1.63	-1.47
<u>Ant[Zn(II)TrNPc]<sub>2</sub> [126]</u>		
[Zn(II)Pc(-1)] <sub>2</sub> /[Zn(II)Pc(-1).Zn(II)Pc(-2)]	0.57	0.56
[Zn(II)Pc(-1).Zn(II)Pc(-2)]/[Zn(II)Pc(-2)] <sub>2</sub>	0.36	0.35
[Zn(II)Pc(-2)] <sub>2</sub> /[Zn(II)Pc(-2).Zn(II)Pc(-3)]	-1.05 <sup>a</sup>	
[Zn(II)Pc(-2)] <sub>2</sub> /[Zn(II)Pc(-3)] <sub>2</sub>		-1.01
[Zn(II)Pc(-2).Zn(II)Pc(-3)]/[Zn(II)Pc(-3)] <sub>2</sub>	-1.31 <sup>a</sup>	
[Zn(II)Pc(-3)] <sub>2</sub> /[Zn(II)Pc(-4)] <sub>2</sub>		-1.53
<u>Nap[Zn(II)TrNPc]<sub>2</sub> [123]</u>		
[Zn(II)Pc(0)] <sub>2</sub> /[Zn(II)Pc(-1)] <sub>2</sub>	1.22 <sup>a</sup>	1.11
[Zn(II)Pc(-1)] <sub>2</sub> /[Zn(II)Pc(-1).Zn(II)Pc(-2)]	0.56	0.59
[Zn(II)Pc(-1).Zn(II)Pc(-2)]/[Zn(II)Pc(-2)] <sub>2</sub>	0.35	0.41
[Zn(II)Pc(-2)] <sub>2</sub> /[Zn(II)Pc(-3)] <sub>2</sub>	-1.18 (-1.34 <sup>b</sup> )	-1.07
[Zn(II)Pc(-3)] <sub>2</sub> /[Zn(II)Pc(-4)] <sub>2</sub>	-1.53	-1.45
<u>[Zn(II)TrNPc]<sub>4</sub> [65]</u>		
[Zn(II)Pc(-1)] <sub>2</sub> /[Zn(II)Pc(-1).Zn(II)Pc(-2)]	0.53	0.58
[Zn(II)Pc(-1).Zn(II)Pc(-2)]/[Zn(II)Pc(-2)] <sub>2</sub>	0.42	0.43
[Zn(II)Pc(-2)] <sub>2</sub> /[Zn(II)Pc(-3)] <sub>2</sub>	-1.15	-1.04
[Zn(II)Pc(-3)] <sub>2</sub> /[Zn(II)Pc(-4)] <sub>2</sub>	-1.64	-1.46
<u>Nap[Co(II)TrNPc]<sub>2</sub> [123]</u>		
[Co(III)Pc(-1).Co(III)Pc(-2)]/[Co(III)Pc(-2)] <sub>2</sub>	----	0.81 <sup>d</sup>
[Co(III)Pc(-2)] <sub>2</sub> /[Co(III)Pc(-2).Co(II)Pc(-2)]	----	0.69
[Co(III)Pc(-1)] <sub>2</sub> /[Co(II)Pc(-1)] <sub>2</sub> (?)	1.02	----

211

Species	$E_{1/2}/V$ DCB	$E_{1/2}/V$ DMF
$[Co(II)Pc(-1)]_2/[Co(II)Pc(-1).Co(II)Pc(-2)]$	0.63	----
$[Co(II)Pc(-1).Co(II)Pc(-2)]/[Co(II)Pc(-2)]_2$	0.49	----
$[Co(III)Pc(-2).Co(II)Pc(-2)]/[Co(II)Pc(-2)]_2$	----	0.45
$[Co(II)Pc(-2)]_2/[Co(II)Pc(-2).Co(I)Pc(-2)]$	-0.41	-0.47
$[Co(II)Pc(-2).Co(I)Pc(-2)]/[Co(I)Pc(-2)]_2$	-0.80 <sup>c,d</sup>	-0.69 <sup>c,d</sup>
$[Co(I)Pc(-2)]_2/[Co(I)Pc(-3)]_2$	-1.59	-1.57
<b><u>Ant[CoTrNPc]<sub>2</sub> [126]</u></b>		
$[Co(III)Pc(-2)]_2/[Co(III)Pc(-2).Co(II)Pc(-2)]$	-----	0.62
$[Co(II)Pc(-1)]_2/[Co(II)Pc(-1).Co(II)Pc(-2)]$	0.55	-----
$[Co(III)Pc(-2).Co(II)Pc(-2)]/[Co(II)Pc(-2)]_2$	-----	0.41
$[Co(II)Pc(-1).Co(II)Pc(-2)]/[Co(II)Pc(-2)]_2$	0.38	-----
$[Co(II)Pc(-2)]_2/[Co(II)Pc(-2).Co(I)Pc(-2)]$	-0.29	-0.20
	-0.42	-----
$[Co(I)Pc(-2).Co(II)Pc(-2)]/[Co(I)Pc(-2)]_2$	-0.77 <sup>c,d</sup>	
	-0.60 <sup>c,d</sup>	
$[Co(I)Pc(-2)]_2/[Co(I)Pc(-3)]_2$	-1.58	-1.48
<b><u>Nap[Cu(II)TrNPc]<sub>2</sub> [123]</u></b>		
$[Cu(II)Pc(0)]_2/[Cu(II)Pc(-1)]_2$	1.23 <sup>c</sup>	
$[Cu(II)Pc(-1)]_2/[Cu(II)Pc(-1).Cu(II)Pc(-2)]$	0.76	0.81 <sup>c</sup>
$[Cu(II)Pc(-1).Cu(II)Pc(-2)]/[Cu(II)Pc(-2)]_2$	0.56	0.51
$[Cu(II)Pc(-2)]_2/[Cu(II)Pc(-3)]_2$	-1.09	-0.88
$[Cu(II)Pc(-3)]_2/[Cu(II)Pc(-4)]_2$	-1.40	-1.32

$E_{1/2}$  values were measured by cyclic voltammetry at 200, 100, 50 and 20 mV/s. Average data  $E_{1/2} = (E_{pa} + E_{pc})/2$  are reported. Hatched lines indicate that the specific redox couple is not permissible in that solvent. <sup>a</sup> Assignment unproven. <sup>b</sup> weak or broad couples of uncertain potential. <sup>c</sup> irreversible. <sup>d</sup> Data obtained from differential pulse voltammetry. <sup>e</sup> Weak peaks, provenance and validity uncertain. Overall charges omitted for clarity.

In general, the stability of mixed-valence phthalocyanines, as defined by the electrochemical splitting or  $K_c$  values, is somewhat larger than for the corresponding porphyrins (to the extent that such comparisons can be made).



Table 10 Comproportionation Data [65, 69, 123, 126]

	Couple <sup>a</sup>	Solvent	E(V) <sup>b</sup>	K <sub>c</sub> <sup>c</sup>	K <sub>d</sub> <sup>d</sup>	ΔG/ kJmol <sup>-1</sup>
Ant[CoTrNPc] <sub>2</sub>	I	DCB	0.17	8.4x10 <sup>2</sup>	1.2x10 <sup>-3</sup>	-17
	II	DCB	0.48	1.8x10 <sup>8</sup>	5.6x10 <sup>-9</sup>	-47
	III	DMF	0.23	9.0x10 <sup>3</sup>	1.1x10 <sup>-4</sup>	-23
	II	DMF	0.30	1.4x10 <sup>5</sup>	7.0x10 <sup>-6</sup>	-29
Nap[CoTrNPc] <sub>2</sub>	I	DCB	0.14	2.8x10 <sup>2</sup>	2.5x10 <sup>-3</sup>	-14
	II	DCB	0.39	4.0x10 <sup>6</sup>	2.5x10 <sup>-7</sup>	-38
	III	DMF	0.24	1.3x10 <sup>4</sup>	7.5x10 <sup>-5</sup>	-24
	II	DMF	0.22	6.1x10 <sup>3</sup>	1.65x10 <sup>-4</sup>	-22
EtMeO(5)- [ZnTrNPc] <sub>2</sub>	I	DCB	0.08	2.4x10 <sup>1</sup>	4.2x10 <sup>-2</sup>	-8
	I	DMF	0.15	3.8x10 <sup>2</sup>	2.6x10 <sup>-3</sup>	-15
[ZnTrNPc] <sub>4</sub>	I	DCB	0.11	7.8x10 <sup>1</sup>	1.3x10 <sup>-2</sup>	-11
	I	DMF	0.15	3.8x10 <sup>2</sup>	2.6x10 <sup>-3</sup>	-15
Ant[ZnTrNPc] <sub>2</sub>	I	DCB	0.21	4.1x10 <sup>3</sup>	2.45x10 <sup>-4</sup>	-21
	I	DMF	0.21	4.1x10 <sup>3</sup>	2.45x10 <sup>-4</sup>	-21
Nap[ZnTrNPc] <sub>2</sub>	I	DCB	0.21	4.1x10 <sup>3</sup>	2.45x10 <sup>-4</sup>	-21
	I	DMF	0.18	1.2x10 <sup>3</sup>	8.0x10 <sup>-4</sup>	-18
Nap[CuTrNPc] <sub>2</sub>	I	DCB	0.20	2.7x10 <sup>3</sup>	3.6x10 <sup>-4</sup>	-20
(-1)[ZnTrNPc] <sub>2</sub>	I	DCB	0.26	2.95x10 <sup>4</sup>	3.4x10 <sup>-5</sup>	-25
	I	DMF	0.22	6.1x10 <sup>3</sup>	1.65x10 <sup>-4</sup>	-22
FAIPc-O-PcAlF	I	DMF	0.40	6.0x10 <sup>6</sup>	1.7x10 <sup>-7</sup>	-39
RSiPc-O-PcSiR	I <sup>e</sup>	CH <sub>2</sub> Cl <sub>2</sub>	0.49	2.7x10 <sup>8</sup>	3.7x10 <sup>-9</sup>	-49
	IV	CH <sub>2</sub> Cl <sub>2</sub>	0.40	7.6x10 <sup>6</sup>	1.3x10 <sup>-7</sup>	-40
FePc-O-PcFe	III <sup>f</sup>	Py	0.36	1.3x10 <sup>6</sup>	7.7x10 <sup>-7</sup>	-35
	V	Py	0.40	6.0x10 <sup>6</sup>	1.7x10 <sup>-7</sup>	-39
FePc-N-PcFe	III <sup>g</sup>	Py	0.27	3.7x10 <sup>4</sup>	2.7x10 <sup>-5</sup>	-26
	V <sup>g</sup>	Py	0.83	1.2x10 <sup>14</sup>	8.3x10 <sup>-15</sup>	-80

<sup>a</sup> I: [MPc(-1)]<sub>2</sub> + [MPc(-2)]<sub>2</sub> → 2[MPc(-1).MPc(-2)]. II: [Co(I)Pc(-2)]<sub>2</sub> + [Co(II)Pc(-2)]<sub>2</sub> → 2[Co(I)Pc(-2).Co(II)Pc(-2)]; III: [M(II)Pc(-2)]<sub>2</sub> + [M(III)Pc(-2)]<sub>2</sub> → 2[M(II)Pc(-2).M(III)Pc(-2)]; IV: [RSiPc(-2)]<sub>2</sub> + [RSiPc(-3)]<sub>2</sub> → 2[RSiPc(-2).RSiPc(-3)] (with oxygen bridge linking silicon atoms). V: [M(III)Pc(-2)]<sub>2</sub> + [M(IV)Pc(-2)]<sub>2</sub> → 2[M(III)Pc(-2).M(IV)Pc(-2)] (with oxygen atoms bridging the iron atoms). For the cobalt complexes, data refer to the *syn* isomer. <sup>b</sup> mixed-valence splitting energy. <sup>c</sup> Comproportionation constant. <sup>d</sup> Disproportionation constant, 1/K<sub>c</sub>. <sup>e</sup> R = n-C<sub>6</sub>H<sub>13</sub>, oxygen bridges axially link the silicon atoms. <sup>f</sup> Oxygen bridges axially link the iron atoms. <sup>g</sup> nitrogen bridges axially link the iron atoms.

- orig fig in  
camera ready  
copy to  
publisher

Figure 12 Hammett Sigma Plot for Substituted Phthalocyanines. Data for metal-free, zinc and cobalt species with redox processes as noted.

This is probably due to the "flatness" of the main phthalocyanine ring system, allowing for closer contact than is usually possible with the more ruffled and often highly substituted porphyrin derivatives.

#### ix. Hammett Relationships

An earlier study [120] showed relationships between the individual Hammett  $\sigma$ (para) parameter [135, 136]] and oxidation potentials for some tetra- and octasubstituted phthalocyanines. In Figure 12 are shown correlations for a range of redox processes for metal free, cobalt, and zinc phthalocyanines as a function of the total,  $\Sigma\sigma$ , value, accounting, thereby, for the number of substituents in the phthalocyanine ring [122].

Since the ring is both meta and para substituted, the use of the para parameter leads to some error. Moreover, although solvent effects in phthalocyanine redox processes are generally small, they are present; it is

therefore not surprising that the data show some scatter. Overall, however, it is clear that, not surprisingly, roughly linear correlations are observed. Moreover for the limited data set shown here, the slopes do not differ greatly. Thus Figure 12 displays two oxidation data sets [Pc(-1)/Pc(-2)], both with slope 0.15 and three (first) reduction data sets, all with slope 0.10. If one may assume that these slopes apply generally to all metallophthalocyanines then it becomes possible to calculate, for example, the oxidation potential of any particular substituted metallophthalocyanine from  $E(\text{ox}) = 0.15\Sigma\sigma + C$ . The value of C is obtained by fitting some known experimental points for the metallophthalocyanine concerned.

---

## F. Conclusions

This review has summarized and discussed the solution electrochemical behavior of a series of metallophthalocyanines with central ions encompassing the whole Periodic Table. The electrochemical versatility of these species, for example, the ability to tune potentials to where they might be useful in an electronic device, by changing metal ion or substituent, makes them potentially extremely valuable in the expanding field of molecular electronics. Such value is enhanced by their overall chemical and thermal stability and usual nontoxicity.

The review has also brought out major gaps in our knowledge of these systems, especially in the left-hand transition groups, and some of the heavier main group species. Greater effort should be expended in synthesizing organic solvent soluble examples of these species. The chemistry of the higher oxidation states of complexes such as molybdenum, tungsten, tin, and bismuth may prove especially illuminating.

A future article in this series will explore the surface electrochemistry and electrocatalytic properties of these fascinating materials.

---

## Acknowledgement

ABPL is indebted to Professor C. C. Leznoff for the continuing collaboration, which has been so productive for the past 12 years, and to all those who have worked upon phthalocyanine chemistry in the Lever and Leznoff laboratories. He is also indebted to the Natural Science and Engineering Research Council (Ottawa) and the Office of Naval Research (Washington) for their continuing financial support.

Table 11 Phthalocyanine and Solvent Abbreviations used in this chapter

Mononuclear phthalocyanines:

DsPc	DisulfonylPc	TNPc	Tetraneopentoxypc
TBPc	Tetra-t-butylPc	TAPc	TetraaminoPc
TcPc	TetracarboxyPc	TEtPc	Tetra-ethylPc
TsPc	TetrasulfonylPc	TBPc	Tetra-t-butylPc
TMxPc	TetramethoxyPc	TNO2Pc	TetranitroPc
OCPc	OctacarboxyPc	OMPc	OctamethylPc
OBuxPc	OctabutoxyPc	OMxPc	OctamethoxyPc
Cl <sub>16</sub> Pc	HexadecachloroPc	OCNPc	OctacyanoPc
TNO2Pc	TetranitroPc		

Binuclear phthalocyanines.

Each of the following species contains three benzene rings each with a substituted neopentox group (abbreviated TrNPc), while the fourth ring is linked by the bridge as described. A number in parenthesis indicate the number of bridging atoms.

O(1)[MTrNPc]<sub>2</sub> an -O- ether link.

C(2)[MTrNPc]<sub>2</sub> -CH<sub>2</sub>-CH<sub>2</sub>- link.

Cat(4)[MTrNPc]<sub>2</sub> a 1,2-catecholate link.

EtMeO(5)[MTrNPc]<sub>2</sub> a diether linkage EtC(Me)(CH<sub>2</sub>OPc)CH<sub>2</sub>OPc.

Nap[MTrNPc]<sub>2</sub> a 1,8-naphthalene direct link.

Ant[MTrNPc]<sub>2</sub> a 1,8-anthracene direct link.

(-1)[MTrNPc]<sub>2</sub> the fourth rings of each phthalocyanine are 3,4- fused.

[MTrNPc]<sub>4</sub> a C(O)<sub>4</sub> spiro tetra-ether linked (tetranuclear) phthalocyanine.

Common solvent abbreviations

ACN acetonitrile; ClN chloronaphthalene; DCB o-dichlorobenzene; DCE 1,2-dichloroethane; DMA dimethylacetamide; DMF dimethylformamide; DMSO dimethylsulfoxide; MeNp methylnaphthalene; PhCN benzonitrile; PhNO<sub>2</sub> nitrobenzene; Py pyridine; THF tetrahydrofuran.

---

## References

1. A. B. P. Lever, Chemtech, 17 (1987) 506.
2. J. F. Myers, G. W. Rayner Canham, and A. B. P. Lever, Inorg. Chem., 14 (1975) 461
3. D. W. Clack and J. R. Yandle, Inorg. Chem., 11 (1972) 1738.
4. D. W. Clack, N. S. Hush, and I. S. Woolsey, Inorg. Chim. Acta, 19 (1976) 129
5. L. D. Rollmann and R. T. Iwamoto, J. Am. Chem. Soc., 90 (1968) 1455.
6. A. B. P. Lever, S. Licoccia, K. Magnell, P. C. Minor, and B. S. Ramaswamy, Adv. Chem. Ser. 201 (1982) 237.
7. A. B. P. Lever, S. R. Pickens, P. C. Minor, S. Licoccia, B. S. Ramaswamy, and K. Magnell, J. Am. Chem. Soc., 103 (1981) 6800.
8. T. Nyokong, Z. Gasyna, and M. J. Stillman, Inorg. Chem., 26 (1987) 1087.
9. M. El Meray, A. Louati, J. Simon, A. Giraudeau, M. Gross, T. Malinski, and K. M. Kadish, Inorg. Chem., 23 (1984) 2606.
10. A. B. P. Lever, M. R. Hempstead, C. C. Leznoff, W. Liu, M. Melnik, W. A. Nevin, and P. Seymour, Pure and Appl. Chem., 58 (1986) 1467.
11. W. Liu, M. R. Hempstead, W. A. Newin, M. Melnik, A. B. P. Lever, and C. C. Leznoff, J. Chem. Soc., Dalton Trans., (1987) 2511.
12. D. Dolphin, B. R. James, A. J. Murray, and J. R. Thornback, Can. J. Chem., 58 (1980) 1125.
13. C. C. Leznoff, S. M. Marcuccio, S. Greenberg, A. B. P. Lever, and K. B. Tomer, Can. J. Chem., 63 (1985) 133.
14. J. H. Weber and D. H. Busch, Inorg. Chem., 4 (1965) 469,472.
15. F. H. Moser and A. L. Thomas, 'The Phthalocyanines', CRC Press, Boca Raton, Florida, 1983, Vol. 1,2
16. R. J. Blagrove, Austr. J. Chem., 26 (1973) 1545.
17. H. Sigel, P. Waldmeier, and B. Prijs, Inorg. Nucl. Chem. Lett., 7 (1971) 161.
18. A. B. P. Lever, Adv. Inorg. Chem. Radiochem., 7 (1965) 27; B. D. Berezin, "Coordination Compounds of Porphyrins and Phthalocyanines", Wiley, New York, 1981; F. H. Moser and A. L. Thomas, 'Phthalocyanine Compounds', Reinhold Publ. Corp., New York, 1963
19. A. J. Bard and L. J. Faulkner, "Electrochemical Methods", John Wiley, New York, 1980.
20. M. Nicholson, in this volume, Chapter 5.
21. K. M. Kadish, Progr. Inorg. Chem., 34 (1986) 435.
22. K. M. Kadish, Q. Y. Xu, and J. E. Anderson, ACS Symp. Ser. Vol. 378 (1988) 451.
23. K. M. Kadish, Chem. Rev., 88 (1988) 1121.
24. M. Gouterman in "The Porphyrins", ed. D. Dolphin, Academic Press, New

- York, 1978, Vol. 1, p.1; A. M. Schaffer, M. Gouterman, and E. R. Davidson, Theor. Chim. Acta, 30 (1973) 9.
25. L. Edwards and M. Gouterman, J. Mol. Spectrosc., 33 (1970) 292.
26. M. Gouterman, G. H. Wagniere, and L. C. Snyder, Jr., J. Mol. Spectrosc., 11 (1963) 2.
27. C. Weiss, H. Kobayashi, and M. Gouterman, J. Mol. Spectrosc., 16 (1965) 415.
28. A. J. McHugh, M. Gouterman, and C. Weiss, Theor. Chim. Acta, 24 (1972) 346.; A.M.Schaffer and M. Gouterman, Theor. Chim. Acta, 25 (1972) 62.
29. M. J. Stillman and T. Nyokong, in "Phthalocyanines, Properties and Applications", vol. 1, p. 133.
30. P. C. Minor, M. Gouterman, and A. B. P. Lever, Inorg. Chem., 24 (1985) 1894.
31. D. Wohrle and G. Meyer, Kontakte (Darmstadt), 3 (1985) 38.
32. N. S. Hush and A. S. Cheung, Chem. Phys. Lett., 47 (1977) 1; D. W. Clack, N. S. Hush and J. R. Yandle, Chem. Phys. Lett., 1 (1967) 157.
33. A. Louati, M. El Meray, J. J. Andre, J. Simon, K. M. Kadish, M. Gross, and A. Giraudeau, Inorg. Chem., 24 (1985) 1175.
34. D. J. E. Ingram and J. E. Bennett, J. Chem. Phys., 22 (1954) 1136.
35. F. H. Winslow, W. O. Baker, and W. A. Yager, J. Am. Chem. Soc., 77 (1955) 4751.
36. T. Fu Yen, J. G. Erdman, and A. J. Saraceno, Anal. Chem., 34 (1962) 694.
37. S. E. Harrison and J. M. Assour, J. Chem. Phys., 40 (1964) 365.
38. J. M. Assour and S. E. Harrison, J. Chem. Phys., 68 (1964) 872.
39. J. F. Boas, P. E. Fielding, and A. G. Mackay, Austr. J. Chem., 27 (1974) 7.
40. E. G. Sharoyan, N. N. Tikhomirova, and L. A. Blumenfeld, Zh. Strukt. Khim., 6 (1965) 843.
41. J. B. Raynor, M. Robson, and A. S. M. Torrens-Burton, J. Chem. Soc., Dalton Trans., (1977) 2360.
42. J. R. Harbour and M. J. Walzak, Langmuir, 2 (1986) 788.
43. A. B. P. Lever and P. C. Minor, Inorg. Chem., 20 (1981) 4015.
44. R. D. Shannon and C. T. Prewitt, Acta Crystall., 7 (1965) 27.
45. T. Nyokong, Z. Gasyna, and M. J. Stillman, Inorg. Chem., 26 (1987) 548.
46. R. O. Loutfy and Y. C. Cheng, J. Chem. Phys., 73 (1980) 2902.
47. C. C. Leznoff, S. Greenberg, S. M. Marcuccio, P. C. Minor, P. Seymour, and A. B. P. Lever, Inorg. Chem. Acta, 89 (1984) L35.
48. G. Fu, Y-S. Fu, K. Jayaraj, and A. B. P. Lever, Inorg. Chem., 29 (1990) 4090.
49. W. A. Nevin, M. R. Hempstead, W. Liu, C. C. Leznoff, and A. B. P. Lever, Inorg. Chem., 26 (1987) 570.
50. E. P. Platonova, E. Yu. Skuridin, and L. S. Degtyarev, Zh. Obshch. Khim., 54 (1984) 925.
51. S. V. Vulfson, O. L. Kaliya, O. L. Lebedev, and E. A. Luk'yanets, Zh. Organ. Khim., 12 (1976) 123.

52. R. H. Campbell, G. A. Heath, G. T. Hefter, and R. C. S. McQueen, J. Chem. Soc., Chem. Commun., (1983) 1123.
53. R. O. Loutfy, personal communication, 1982
54. A. B. P. Lever, S. Licoccia, B. S. Ramaswamy, S. A. Kandil, and D. V. Stynes, Inorg. Chim. Acta, 51 (1981) 169.
55. A. Giraudeau, A. Louati, M. Gross, J. J. Andre, J. Simon, C. H. Su, and K. M. Kadish, J. Am. Chem. Soc., 105 (1983) 2917.
56. H. Homborg and K. S. Murray, Z. Anorg. Allg. Chem., 517 (1984) 149.
57. H. Sugimoto, T. Higashi, and M. Mori, J. Chem. Soc., Chem. Commun. (1983) 622.
58. P. Turek, J.-J. Andre, A. Giraudeau, and J. Simon, Chem. Phys. Lett., 134 (1987) 471.
59. D. Lexa and M. Reix, J. Chim. Phys., 71 (1974) 511.
60. A. Giraudeau, F.-R. F. Fau, and A. J. Bard, J. Am. Chem. Soc., 102 (1980) 5137.
61. A. B. P. Lever and J. P. Wilshire, Can. J. Chem., 54 (1976) 2514.
62. A. Wolberg and J. Manasson, J. Am. Chem. Soc., 92 (1970) 2982.
63. M. N. Golovin, P. Seymour, K. Jayaraj, Y-S. Fu, and A. B. P. Lever, Inorg. Chem., 29 (1990) 1719.
64. J. T. S. Irvine, B. R. Eggins, and J. Grimshaw, J. Electroanal. Chem., 271 (1989) 161.
65. V. Manivannan, W. A. Nevin, C. C. Leznoff, and A. B. P. Lever, J. Coord. Chem., 19 (1988) 139.
66. V. I. Gavrilov, E. A. Luk'yanets, and I. V. Shelepin, Electrokhimiya, 17 (1981) 1183.
67. V. I. Gavrilov, L. G. Tomilova, I. V. Shelepin, and E. A. Luk'yanets, Electrokhimiya, 15 (1979) 1058.
68. D. Wohrle and V. Schmidt, J. Chem. Soc., Dalton Trans., (1988) 549.
69. D. W. DeWulf, J. K. Lelend, B. L. Wheeler, A. J. Bard, D. A. Batzel, D. R. Dininny and M. E. Kenney, Inorg. Chem., 26 (1987) 266.
70. H. Li and T. F. Guarr, J. Chem. Soc., Chem. Commun., (1989) 832.
71. Y. Orihashi, M. Nishikawa, H. Ohno, E. Tsuchida, H. Matsuda, H. Nakanishi, and M. Kato, Bull. Chem. Soc., Jpn., 60 (1987) 3731.
72. C. C. Leznoff, Unpublished work
73. H. Sugimoto, M. Mori, H. Masuda, and T. Taga, J. Chem. Soc., Chem. Commun., (1986) 962.
74. A. B. Anderson, T. L. Gordon, and M. E. Kenney, J. Am. Chem. Soc., 107 (1985) 192.
75. T. M. Mezza, N. R. Armstrong, G. W. Ritter II, J. P. Iafalice, and M. E. Kenney, J. Electroanal. Chem., 137 (1982) 227.
76. B. L. Wheeler, G. Nagasubramanian, A. J. Bard, L. A. Schechtman, D. R. Dininny, and M. E. Kenney, J. Am. Chem. Soc., 106 (1984) 7404.
77. B. Simic-Glavaski, A. A. Tanaka, M. E. Kenney, and E. Yeager, J.

- Electroanal. Chem., 229 (1987) 285.
78. E. Ciliberto, K. A. Doris, W. J. Pietro, G. M. Reisner, D. E. Ellis, I. Fragala, F. H. Herbstein, M. A. Ratner, and T. J. Marks, J. Am. Chem. Soc., 106 (1984) 7748.
79. E. S. Dodsworth, A. B. P. Lever, P. Seymour, and C. C. Leznoff, J. Phys. Chem. 89 (1985) 5698.
80. M. Gouterman, D. Holten, and E. Lieberman, Chem. Phys., 25 (1977) 139.
81. V. R. Shephard, Jr. and N. R. Armstrong, J. Phys. Chem., 83 (1979) 1268.
82. V. I. Gavrilov, A. P. Konstantinov, V. M. Derkacheva, E. A. Luk'yanets, and I. V. Shelepin, Zh. Fiz. Khim., 60 (1986) 1448.
83. V. I. Gavrilov, L. G. Tomilova, V. M. Derkacheva, E. V. Chernykh, N. T. Ioffe, I. V. Shelepin and E. A. Luk'yanets, Zh. Obshch. Khim., 53 (1983) 1347.
84. C. Paliteiro and J. B. Goodenough, J. Electroanal. Chem., 239 (1988) 273.
85. The rest potential is the open circuit potential, when zero current is flowing, that is, no oxidation or reduction chemistry is taking place.
86. A. B. P. Lever, Ph. D. Thesis, London, 1960.
87. T. J. Klofta, J. Danziger, P. Lee, J. Pankow, K. W. Nebesny, and N. R. Armstrong, J. Phys. Chem., 91 (1987) 5646.
88. R. Behnisch and M. Hanack, Synth. Metal, 36 (1990) 387.
89. M. Hanack and A. Datz, Chem. Ber., 119 (1986) 1281.
90. J. E. Elvidge and A. B. P. Lever, J. Chem. Soc., (1961) 1265.
91. This complex was initially identified as Cr(II)[TBuPc(-2)].H<sub>2</sub>O but, given its electrochemical data, it is more likely HOCr(III)[TBuPc(-2)] Previously Unpublished analytical data are: Found C, 71.6; H, 6.4; N, 13.3 Calcd. for HOCr(III)[TBuPc(-2)] C, 71.53; H, 6.13; N, 13.90 %
92. a) A. B. P. Lever and J. P. Wilshire, previously unpublished data; b). T. Nyokong, G. Ferraudi, and M. Feliz, submitted to J. Photochem. Photobiol. 1991.
93. A. B. P. Lever, P. C. Minor, and J. P. Wilshire, Inorg. Chem., 20 (1981) 2550.
94. P. C. Minor and A. B. P. Lever, Inorg. Chem., 22 (1983) 826.
95. A. B. P. Lever and P. C. Minor, Adv. Mol. Relax. Proc., 18 (1980) 115.
96. D. J. Cookson, T. D. Smith, J. F. Boas, P. R. Hicks, and J. R. Pilbrow, J. Chem. Soc., Dalton Trans., (1977) 211.
97. A. B. P. Lever and J. P. Wilshire, Inorg. Chem., 17 (1978) 1145.
98. K. M. Kadish, L. A. Bottomley, and J. S. Cheng, J. Am. Chem. Soc., 100 (1978) 2731.
99. M. Mossayan-Deneux and D. Benlian, J. Inorg. Nucl. Chem., 43 (1981) 635.
100. W. Kalz, H. Homborg, H. Kuppers, B. J. Kennedy, and K. S. Murray, Z. Naturforsch., B 39b (1984) 1478.
101. W. A. Nevin, W. Liu, M. Melnik, and A. B. P. Lever, J. Electroanal. Chem., 213 (1986) 217.
102. M. Brezina, W. Khalil, J. Koryta, and M. Musilova, J. Electroanal. Chem., 77



- (1977) 237.
103. R. S. Nicholson and I. Shain, Anal. Chem., 36 (1964) 706.
104. E. Ough, T. Nyokong, K. A. M. Creber, and M. J. Stillman, Inorg. Chem., 27 (1988) 2724.
105. Y. Orihashi, H. Ohno, E. Tsuchida, H. Matsuda, H. Nakanishi, and M. Kato, Chem. Lett., (1987) 601.
106. L. A. Bottomley, C. Ercolani, J. -N. Gorce, G. Pennesi, and G. Rossi, Inorg. Chem., 25 (1986) 2338.
107. M. Hanack, A. Lange, M. Rein, R. Behnisch, G. Renz, and A. Leverenz, Synth. Metal., 29 (1989) F1.
108. G. Ferraudi, S. Oishi, and S. Muraldiharan, J. Phys. Chem., 88 (1984) 5261.
109. Y. H. Tse, L. Persaud, P. Seymour, and A. B. P. Lever, work in progress.
110. J. Ouyang, K. Shigehara, A. Yamada, and F. A. Anson, J. Electroanal. Chem., 297 (1991) 489.
111. L. A. Bottomley, J. -N. Gorce, V. L. Goedken, and C. Ercolani, Inorg. Chem., 24 (1985) 3733.
112. C. Ercolani and B. Floris, this volume, Chapter 1.
113. G. Ferraudi and D. R. Prasard, J. Chem. Soc., Dalton Trans., (1984) 2137.
114. W. A. Nevin, W. Liu, S. Greenberg, M. R. Hempstead, S. M. Marcuccio, M. Melnik, C. C. Leznoff, and A. B. P. Lever, Inorg. Chem., 26 (1987) 891.
115. P. A. Bernstein and A. B. P. Lever, Inorg. Chem., 29 (1990) 608.
116. K. Kusuda, K. Shiraki, and H. Yamaguchi, Ber. Bunsenges. Phys. Chem., 92 (1988) 725.
117. V. I. Gavrilov, L. G. Tomilova, E. V. Chernykh, O. L. Kalija, I. V. Shelepin, and E. A. Luk'yanetz, Zh. Obshch. Khim., 50 (1980) 2143.
118. E. B. Fleischer, S. Jacobs, and L. Mestichelli, J. Am. Chem. Soc., 90 (1968) 2527.
119. C. C. Leznoff, H. Lam, S. M. Marcuccio, W. A. Nevin, P. Janda, N. Kobayashi and A. B. P. Lever, J. Chem. Soc. Chem. Commun., (1987) 699.
120. Y. Orihashi, H. Ohno, and E. Tsuchida, Mol. Cryst. Liq. Cryst., 160 (1988) 139.
121. Y. Orihashi, N. Kobayashi, E. Tsuchida, H. Matsuda, H. Nakanishi, and M. Kato, Chem. Lett., (1985) 1617.
122. A. B. P. Lever, unpublished observations.
123. C. C. Leznoff, H. Lam, W. A. Nevin, N. Kobayashi, P. Janda, and A. B. P. Lever, Angew. Chem. Int. Ed., 26 (1987) 1021.
124. H. C. Brown and Y. Okamoto, J. Am. Chem. Soc., 80 (1958) 4979.
125. M. Hanack, C. Deger, and A. Lange, Coord. Chem. Rev., 83 (1988) 115.
126. N. Kobayashi, H. Lam, W. A. Nevin, P. Janda, C. C. Leznoff, and A. B. P. Lever, Inorg. Chem., 29 (1990) 3415.
127. M. Hanack, and A. Hirsch, Synth. Metal., 19 (1988) 139.
128. G. Rossi, M. Gardini, G. Pennesi, C. Ercolani, and V. L. Goedkin, J. Chem. Soc., Dalton Trans., (1989) 193.

129. K. M. Kadish, R. K. Rhodes, L. A. Bottomley and H. M. Goff, Inorg. Chem., 20 (1981) 3195.
130. C. Ercolani, F. Monacelli, S. Dzugas, V. L. Goedken, G. Pennesi, and G. Rossi, J. Chem. Soc. Dalton Trans., (1991) 1309.
131. A. Beck, M. Hanack, and K. M. Mangold, Chem. Ber., 124 (1991) 2315.
132. A. Leverenz, Ph. D. Thesis, Tübingen, 1990
133. A. MacGrath, C. B. Storm, and W. S. Koski, J. Am. Chem. Soc., 87 (1965) 1470.
134. T. G. Brown and B. M. Hoffman, Mol. Phys., 39 (1980) 103.
135. C. D. Ritchie, "Physical Organic Chemistry", 2nd Edn., Marcel Dekker, NY, 1990.
136. H. C. Brown and Y. Okamoto, J. Am. Chem. Soc., 80 (1958) 4979.
137. M. Hanack, personal communication, 1992.